The Abdus Salam
International Centre for Theoretical Physics

United Nations
Educational, Scientific and
Cultural Organization

IAEA
International Atomic Energy Agency

2292-17

School and Conference on Analytical and Computational Astrophysics

14 - 25 November, 2011

Solar wind modelling

Carla Jacobs
K.U. Leuven, Centre for Plasma Astrophysics, Leuven
Belgium

Solar wind modelling

Carla Jacobs

Centrum voor Plasma-Astrofysica
K.U.Leuven, Belgium

ICTP, Trieste, 22 November 2011

Outline

Outline

Discovery of the solar wind

- 1940's-50's: Systematic deflection of comet tails; they always point away from the Sun.
- Early 1950s: Biermann realises this cannot be explained by the solar radiation pressure.
- Suggests the existence of a continuous solar outflow.

Discovery of the solar wind

In 1958, Parker derived the first theoretical model of the solar wind.

- The solar corona is not in hydrostatic equilibrium $\rightsquigarrow$ non-vanishing pressure at infinity.
- Considered a spherical symmetric, isothermal fluid model in stationary equilibrium.

$$
\begin{aligned}
\frac{1}{r^2}\frac{d}{dr}\left(r^2 \rho v_r\right) &= 0, \\
v_r \frac{dv_r}{dr} &= -\frac{GM}{r^2} - \frac{1}{\rho}\frac{dp}{dr}.
\end{aligned}
$$

Discovery of the solar wind

In 1958, Parker derived the first theoretical model of the solar wind.

- The solar corona is not in hydrostatic equilibrium $\rightsquigarrow$ non-vanishing pressure at infinity.
- Considered a spherical symmetric, isothermal fluid model in stationary equilibrium.

$$\frac{1}{v_r}\left(\frac{v_r^2}{c_s^2}-1\right)\frac{dv_r}{dr}=\frac{2}{r}\left(1-\frac{GM/2c_s^2}{r}\right).$$

- Flow starts subsonic near the solar surface $v_r/c_s < 1$ and $r < GM/2c_s^2 = r_s \Rightarrow dv_r/dr > 0$.
- Flow crosses the sonic point: $v_r = c_s$ in $r = r_s$ and becomes supersonic ($dv_r/dr > 0$).

Discovery of the solar wind

In 1958, Parker derived the first theoretical model of the solar wind.

- Combine with Bernoulli's equation:

$$\frac{v_r^2}{2} - \frac{GM}{r} + \int \frac{dp}{\rho} = E,$$

$$\Downarrow$$

$$\frac{v_r^2}{c_s^2} - \ln \frac{v_r^2}{c_s^2} + \ln \frac{r_s^4}{r^4} - 4\frac{r_s}{r} = H(v_r, r)$$

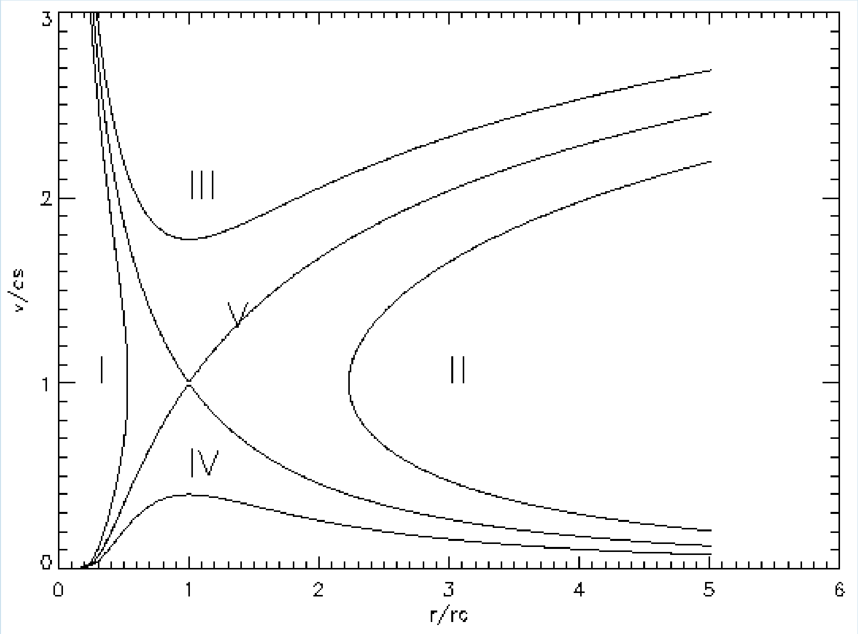

and obtain the transonic solution:

$$\frac{v_r^2}{c_s^2} - \ln \frac{v_r^2}{c_s^2} = -3 - \ln \frac{r_s^4}{r^4} + 4\frac{r_s}{r}.$$

Discovery of the solar wind

In 1958, Parker derived the first theoretical model of the solar wind.

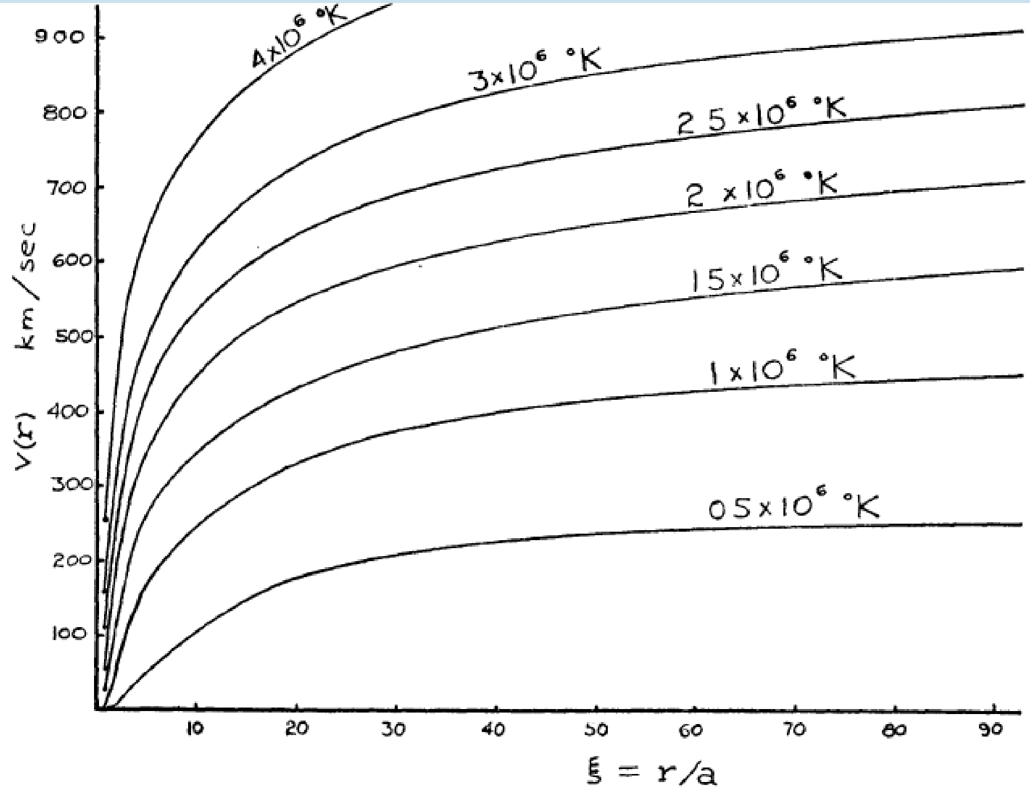

FIG. 1 —Spherically symmetric hydrodynamic expansion velocity $v(r)$ of an isothermal solar corona with temperature T_0 plotted as a function of r/a, where a is the radius of the corona and has been taken to be 10^{11} cm

Discovery of the solar wind

In 1958, Parker derived the first theoretical model of the solar wind.

Parker predicted the existence of a transonic, continuous outflow from the Sun. Few years later it has been detected in-situ by Russian and American space missions.

Observations of the solar wind

What?

- Continuous stream of high energetic particles flowing from the Sun.
- Finds its origin in the hot solar corona: thermally driven wind.
- Two different components:
  - fast ($V > 700$km/s), tenuous, almost uniform stream $\rightarrow$ from coronal holes
  - slow ($V \cong 300$km/s), more dense and turbulent flow $\rightarrow$ from tips and edges of streamers
- Near the Earth: $< V >= 400$km/s, $< n >= 10$cm^{-3}

- $\Rightarrow$ from Ulysses, Helios, ACE, SOHO, Wind, STEREO, etc

Observations of the solar wind

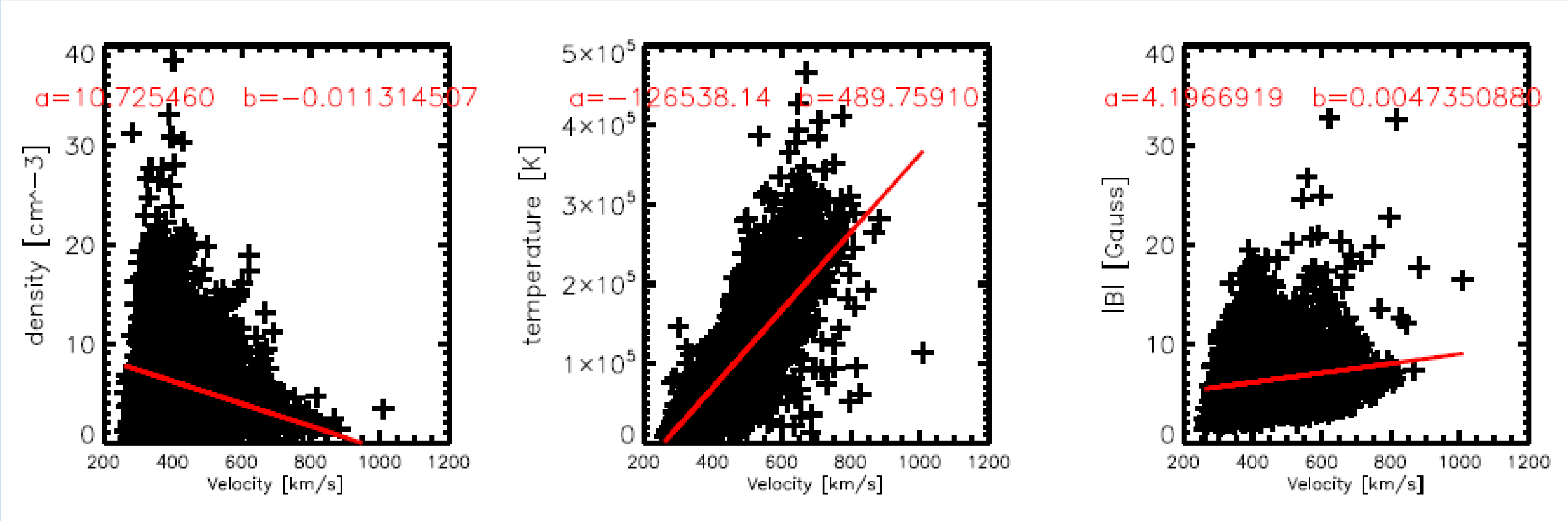

ACE data 1998-2008

Observations of the solar wind

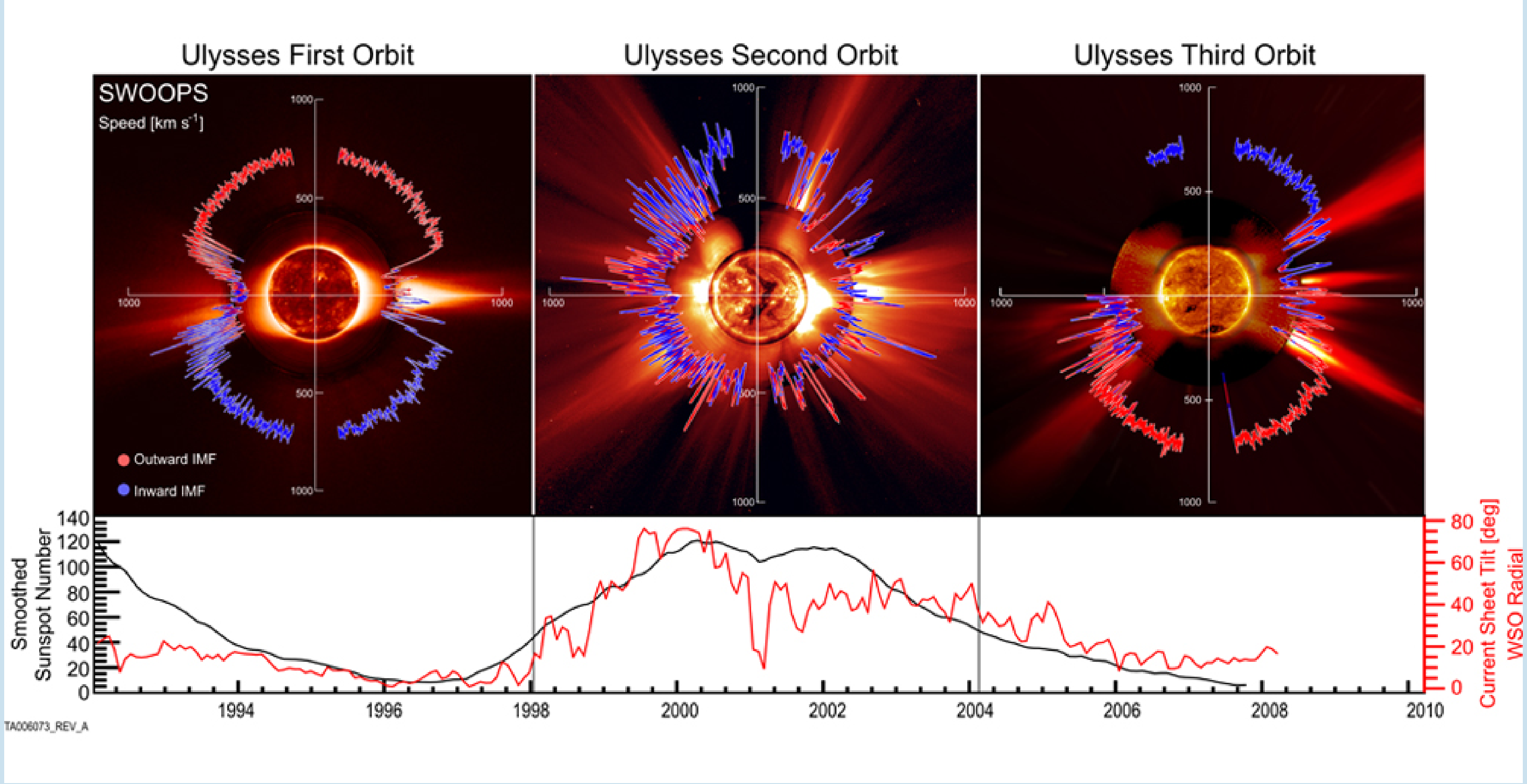

Ulysses, flying in a polar orbit (1990-2009), provided data on the latitudinal and longitudinal dependence of the solar wind speed (red and blue curves). The solar images are from SOHO (ESA/NASA).

Observations of the solar wind

- The solar wind is highly turbulent.
- The magnetic fluctuations show a power law dependence ($f^{-5/3}$).
- High correlation between the magnetic and velocity fluctuations ⇒ indicating Alfvénic nature.

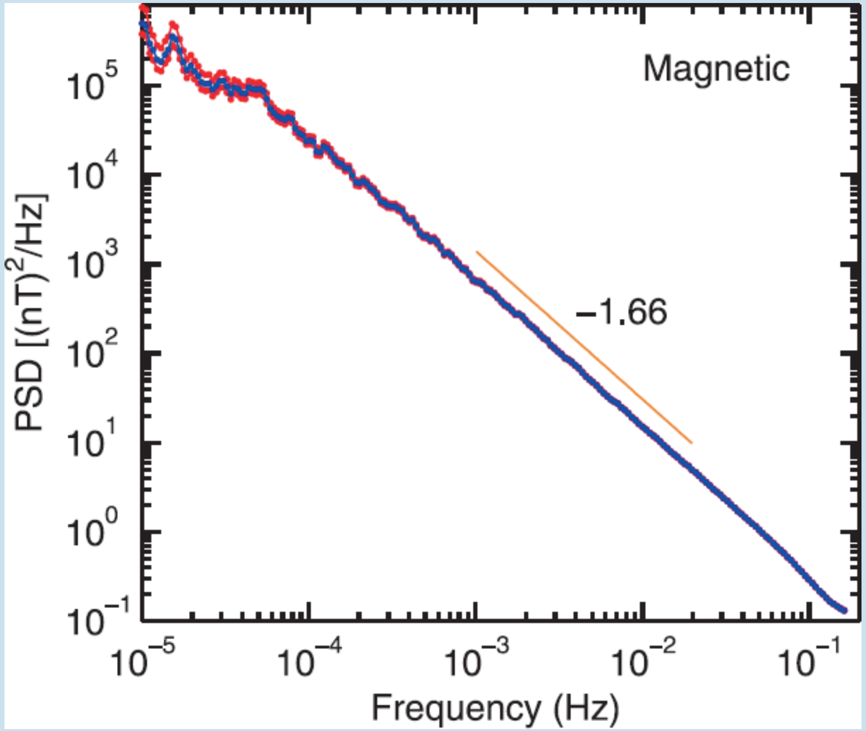

Podesta et al., ApJ 2007

Observations of the solar wind

The solar wind plasma is

- multi-component (protons, electrons, alpha particles and heavier elements)
- not in LTE.
- collisionless.
- strong anisotropy in the velocity distribution functions and temperature.

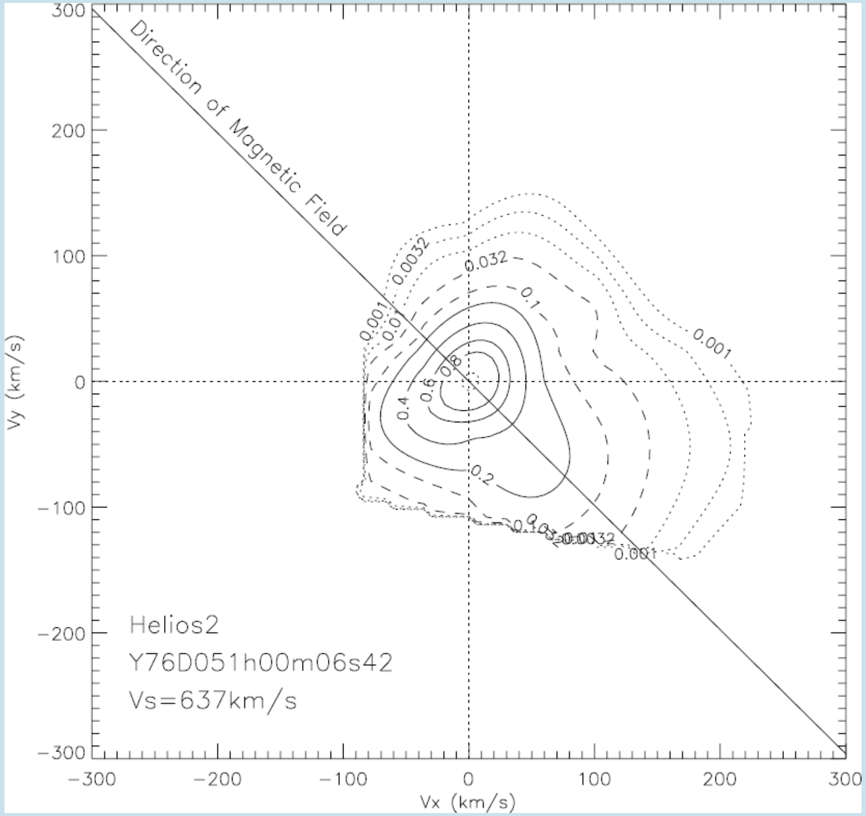

Proton velocity distribution. Marsch et al., JGR 2004

Models for the solar wind

- **Small scale**: kinetic models are used to study the physics of the local heating and dissipation on small spatial-temporal scales. → computationally difficult to include the global structure.
- **Large scale**: fluid models (MHD) can be used to describe the large scale, global behaviour of the solar wind. → no information on the small scale (kinetic) phenomena.

- Ofman, *Wave modelling of the solar wind*, Living Reviews in Solar Physics (2010)
- Marsch, *Kinetic physics of the solar corona and solar wind*, Living Reviews in Solar Physics (2006)

Why modelling the solar wind?

The solar wind is the background medium in which coronal mass ejections propagate $\Rightarrow$ a realistic, time-dependent modelling of the solar wind is essential for space weather forecasting.

Important questions:

- What are the mechanisms causing the heating of the solar corona to its million degree temperature?
- What are the mechanisms accelerating the solar wind to its superfast velocity?

Numerical simulations of the solar wind are complementary to the observations and necessary to develop a better understanding of the effect of the solar wind on the propagation of interplanetary shocks, magnetic clouds, and the effect of corotating interaction regions.

Outline

Outline

Weber and Davis's solution

[Weber and Davis (1967) ApJ, vol. 148, pp.217-227]

- Extension of the Parker model, including rotation, magnetic field.
- 1.5D (equatorial plane, radial + azimuthal motions).
- energy supply characterized by a polytropic index. ($p \sim \rho^\gamma$)

$\rightarrow$ a solution that goes to zero for small r and fits observations at 1 AU, has to pass through three critical points.

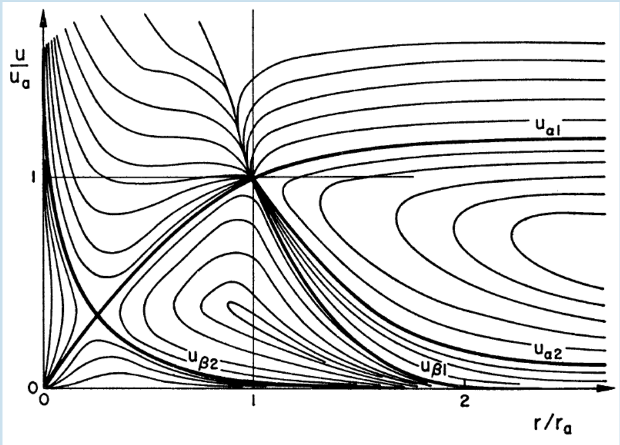

Family of solutions for given γ and r_a

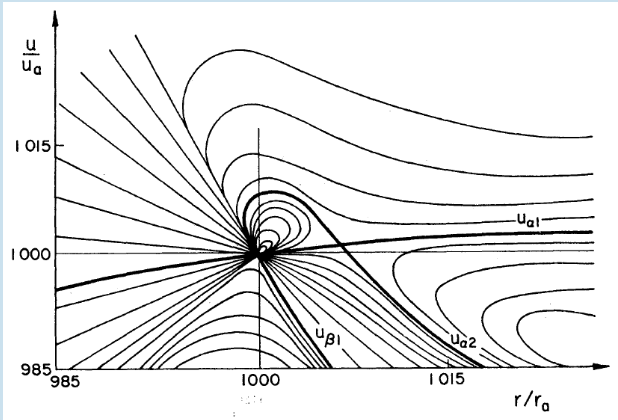

Enlargement near the Alfvénic critical point $r = r_a$

Weber and Davis's solution

[Weber and Davis (1967) ApJ, vol. 148, pp.217-227]

- Extension of the Parker model, including rotation, magnetic field.
- 1.5D (equatorial plane, radial + azimuthal motions).
- energy supply characterized by a polytropic index. ($p \sim \rho^{\gamma}$)

$\rightarrow$ a solution that goes to zero for small r and fits observations at 1 AU, has to pass through three critical points.
$\rightarrow$ 2D generalization by Sakurai (1985)

[Astro. & Astrophys., vol. 152, pp.121-129]

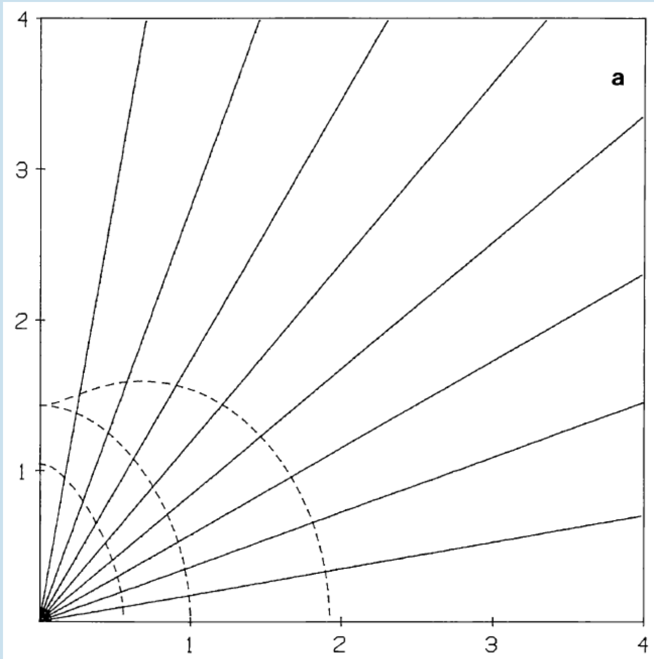

Location of slow, Alfvén, and fast mode critical surfaces for a radial magnetic field (Sakurai '85)

Outline

The computer model of Pneuman & Kopp ('71)

[Pneuman & Kopp (1971) SPh, vol. 18, pp.258-270]

- without rotation, with dipolar magnetic field.
- 2.5D (axi-symm., incl. azimuthal motions).
- isothermal corona.
- closed region: no flow, no radiative nor conductive losses.

→ includes closed field regions and 'helmet' streamer type configuration associated with current sheet!

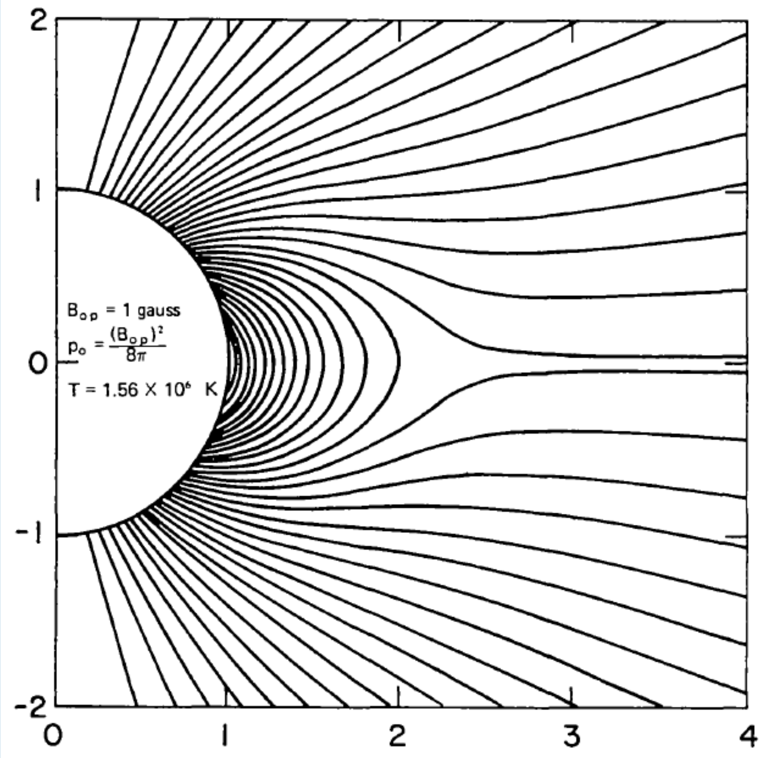

Field and streamline distribution for typical BCs

First 3D MHD model ('88)

[Han, Wu, Dryer (1988) Comp. Fluids, vol. 16, pp.81-103]

- initial steady MHD flow is assumed to be **supersonic and super-Alfvénic** and obtained by
  - dropping time-dependent terms in MHD eqs.
  - Lax-Wendroff finite difference method.
- BCs 18 $R_\odot$: $\rho = 2.35 \times 10^{-9}$ kg/km^3, $V_r = 250$ km/s, $T = 1.1 \times 10^6$ K, etc. $\rightarrow$ representative SW conditions at 1 AU

$\rightarrow$ analyze time-dependent, 3D MHD disturbance propagating through this steady inhomogeneous MHD flow

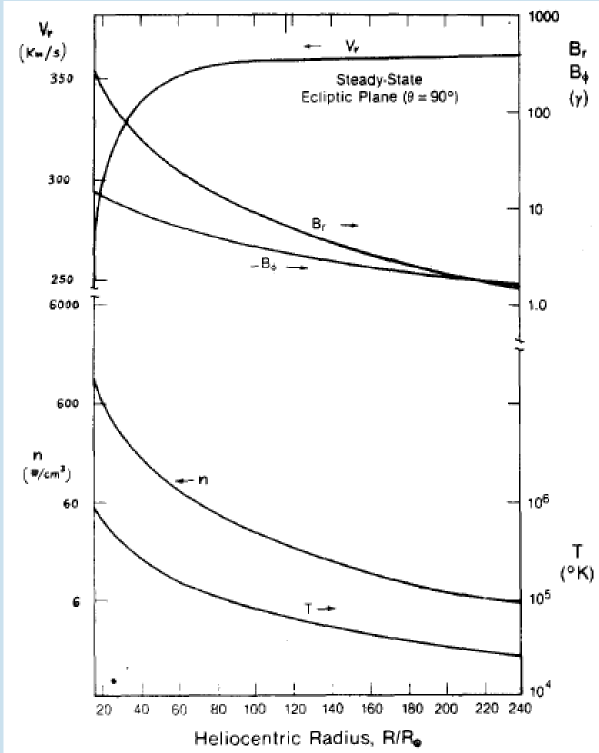

Steady state distributions along r in equatorial plane

Outline

Outline

1. Introduction
2. The ‘early days’
3. The supercomputer era
    - Comparison of axi-symmetric (2.5D) wind models
    - Full 3D solar wind models
4. Conclusions

2.5D solar wind models

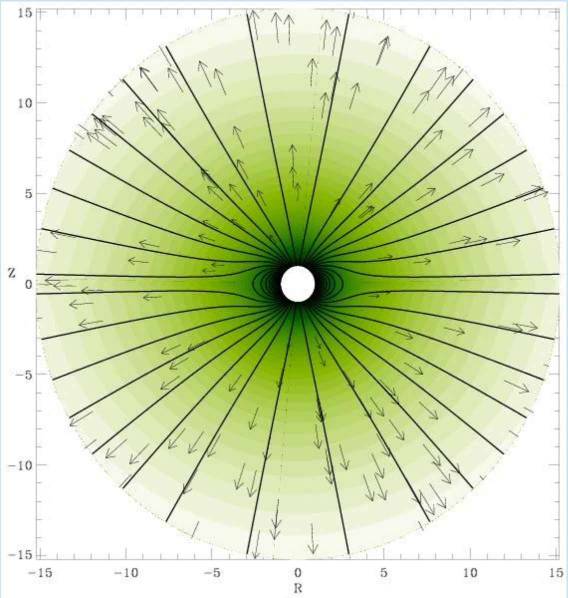

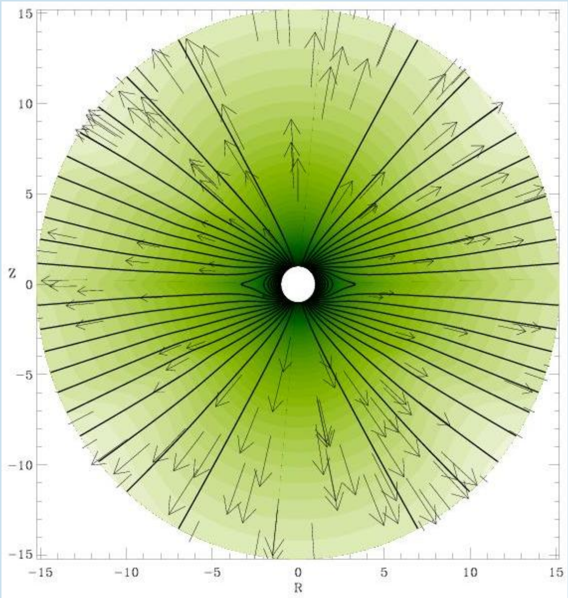

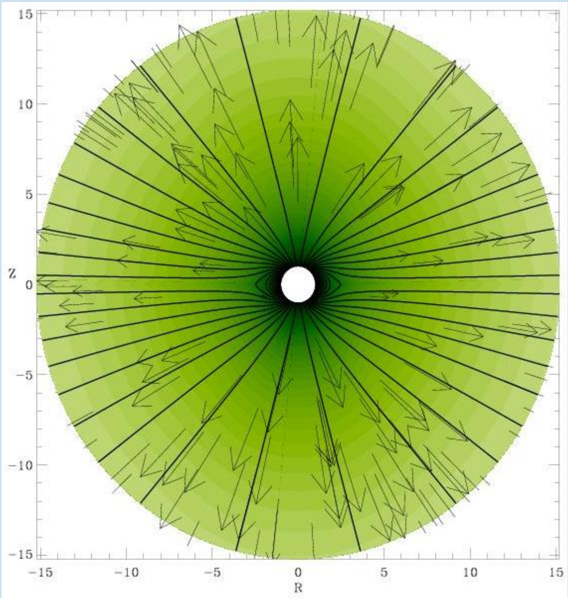

Wind Model 1:
Polytropic Wind $p \sim \rho^{1.05}$
Colour: density (log-scale), black lines: magnetic field lines, arrows: velocity

Wind Model 2:
MHD wind with extra heating source term:
$Q = \rho q_0 e^{-\frac{(r-r_0)^2}{\sigma^2}} \left(T_0 - \gamma \frac{p}{\rho}\right)$
(Groth et al. 2000)

Wind Model 3:
Polytropic Wind with Alfvén Waves
Has additional pressure gradient due to effect of Alfvén waves.

2.5D Solar Wind Models: comparison

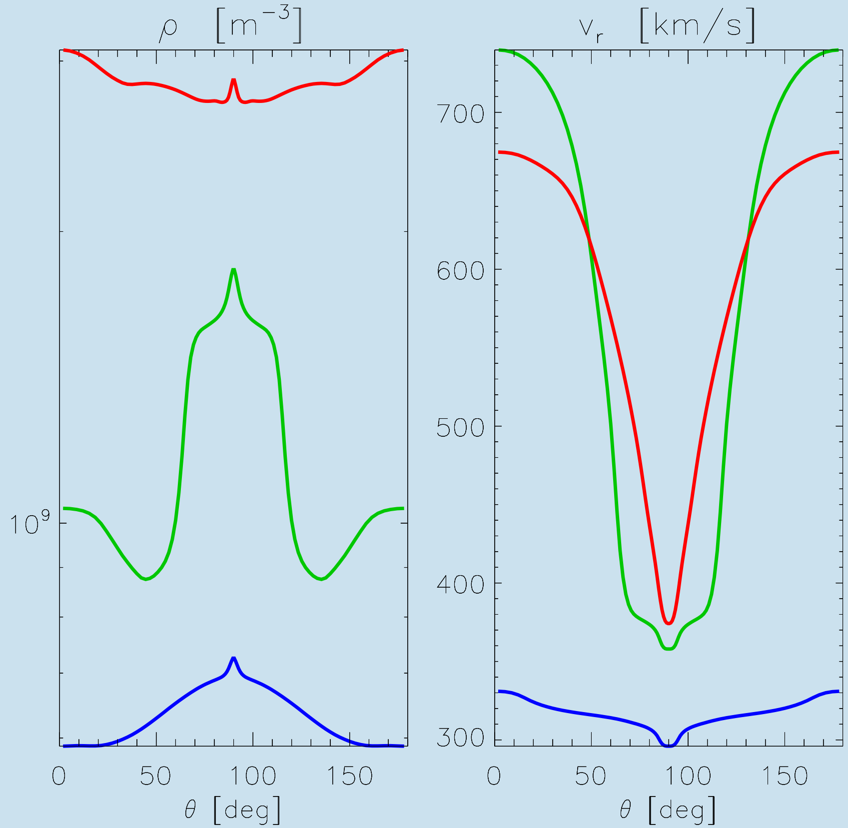

Profiles of density and velocity at $30R_\odot$. Blue: Model 1, green: Model 2, red: Model 3

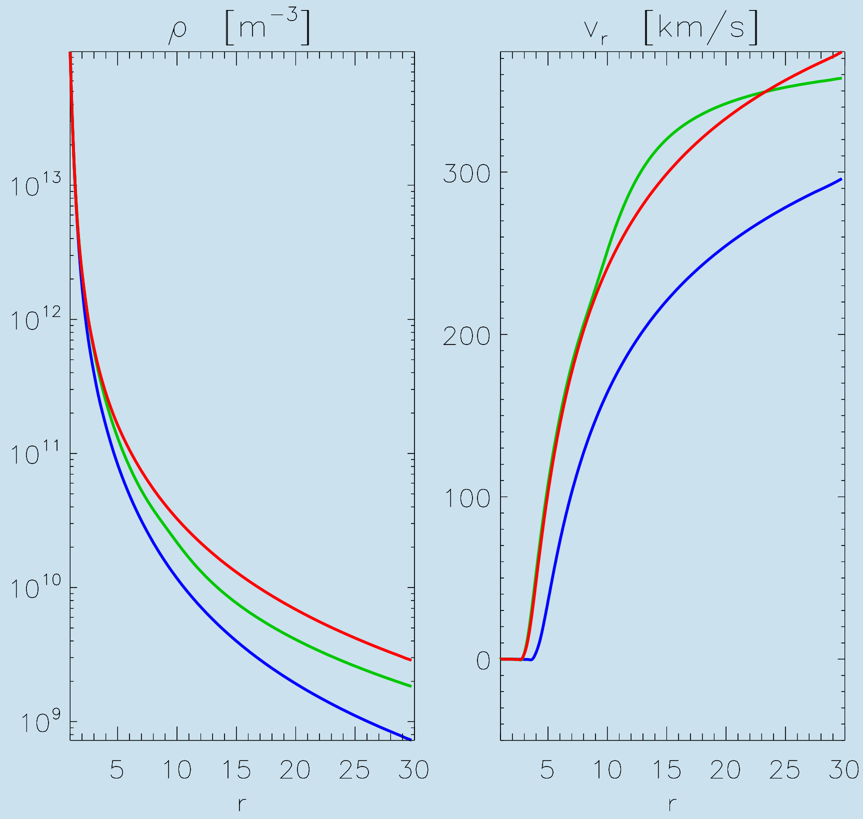

Profiles of density and velocity along the equator. Blue: Model 1, green: Model 2, red: Model 3

2.5D Solar Wind Models: comparison

- Model 1: lowest density, Model 3: highest density
- Model 1: too low velocity, Model 2 & 3: good velocity ratio
- Model 2: sharp gradients because of source term

Outline

1. Introduction
2. The 'early days'
3. The supercomputer era
   - Comparison of axi-symmetric (2.5D) wind models
   - Full 3D solar wind models
4. Conclusions

- 3D simulations are becoming the standard: sufficient computer power.

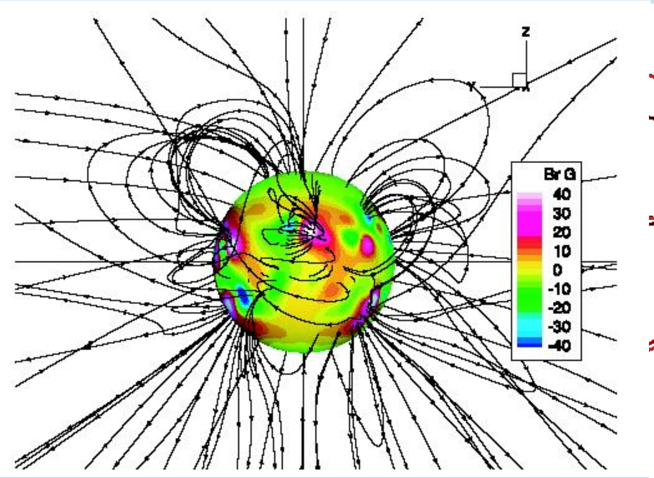

Lugaz et al. 2007

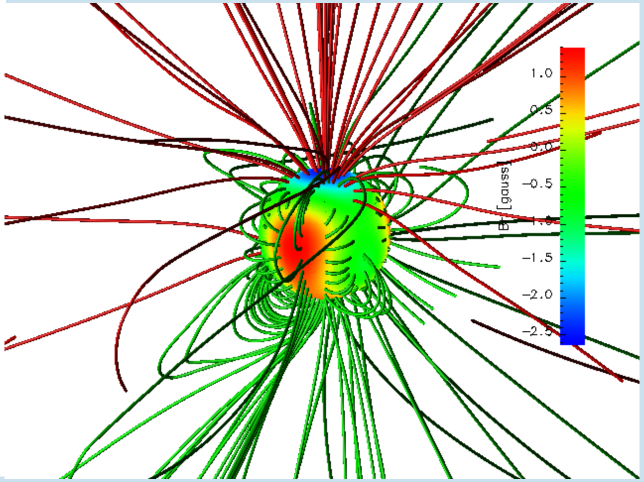

Jacobs 2006

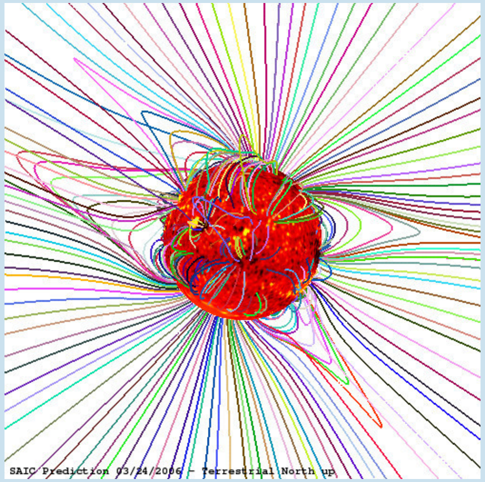

SAIC prediction of the solar corona

- The last decade significant progress had been made in the development of realistic data-driven models for the solar corona/solar wind:

- 3D simulations are becoming the standard: sufficient computer power.
- The last decade significant progress had been made in the development of realistic data-driven models for the solar corona/solar wind:

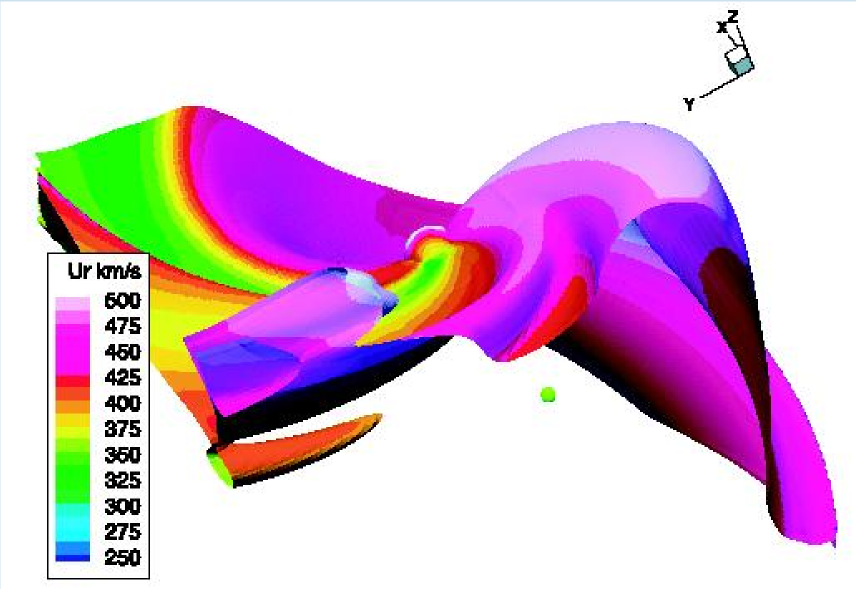

Lugaz et al. 2007, Roussev et al. 2003

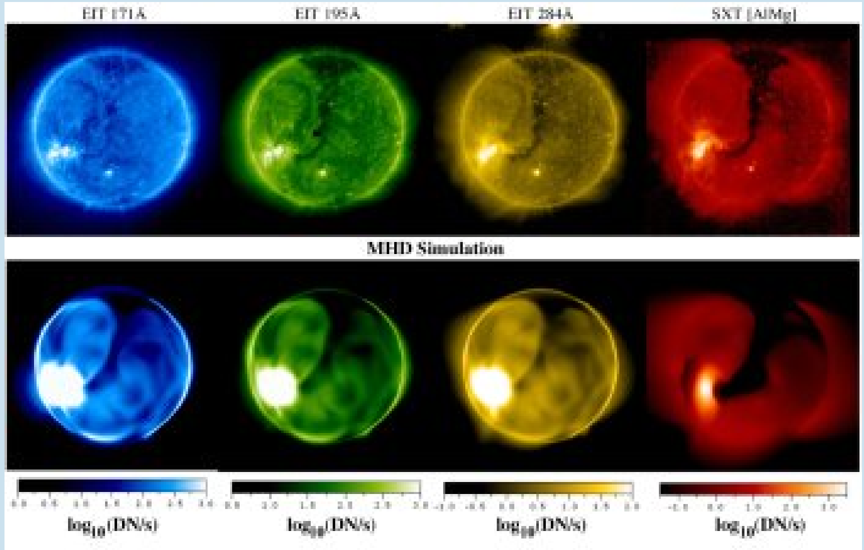

SAIC prediction of the EUV emission during the solar eclipse of March 29, 2006.

MHD model of Linker et al. (1999)

[Linker et al. (1999) JGR, vol. 101, pp.9809-9830]

- use data from Whole Sun Campaign (Aug-Sep, 1996).
- full 3D MHD model **from 1 to 30 $\mathbf{R}_\odot$** (polytropic ($p\rho^{-\gamma}=$const.) with $\gamma = 1.05$)
- **first use of measured phot. field as BC!**

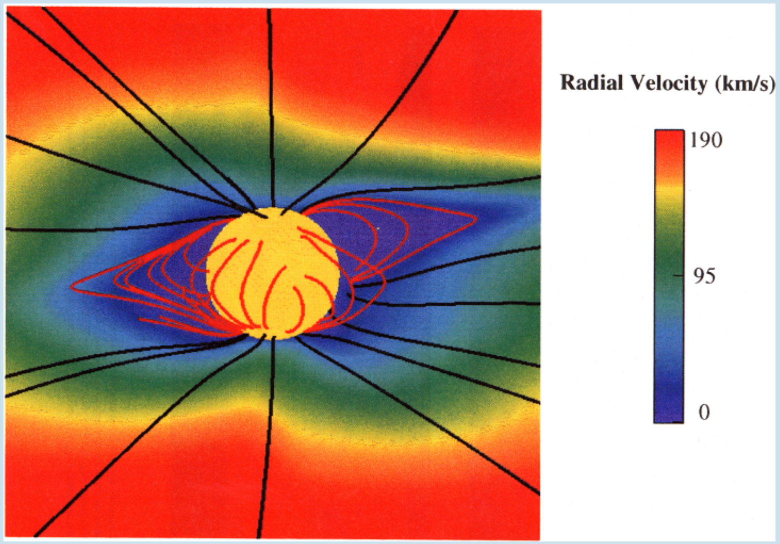

Magnetic field lines superimposed on radial velocity on Sep 3 '96

MHD model of Linker et al. (1999)

[Linker et al. (1999) JGR, vol. 101, pp.9809-9830]

- use data from Whole Sun Campaign (Aug-Sep, 1996).
- full 3D MHD model **from 1 to 30 $\mathbf{R}_{\odot}$** (polytropic ($p\rho^{-\gamma} = \text{const.}$) with $\gamma = 1.05$)
- **first use of measured phot. field as BC!**

$\rightarrow$ comparison with daily and synoptic white light and emission images shows good overall agreement with coronal and IP structures, incl. position and shape of streamer belt

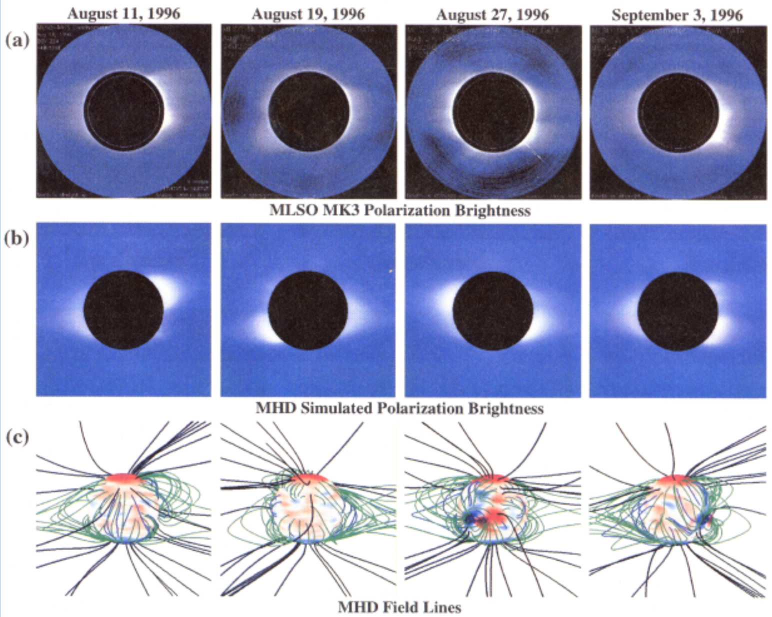

Observed and simulated polarization brightness and magnetic field lines of prediction model

MHD model of Linker et al. (1999)

[Linker et al. (1999) JGR, vol. 101, pp.9809-9830]

- use data from Whole Sun Campaign (Aug-Sep, 1996).
- full 3D MHD model **from 1 to 30 $\mathbf{R}_\odot$** (polytropic ($p\rho^{-\gamma} =$ const.) with $\gamma = 1.05$)
- **first use of measured phot. field as BC!**

$\rightarrow$ comparison with daily and synoptic white light and emission images shows good overall agreement with coronal and IP structures, incl. position and shape of streamer belt

$\rightarrow$ quantitative disagreements exist

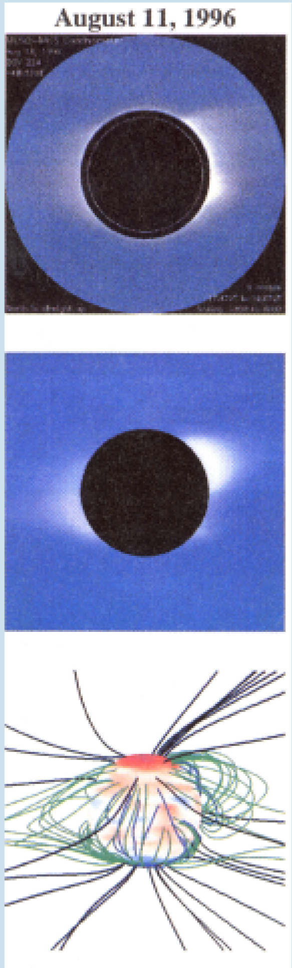

More polytropic wind models

[Hayashi, ApJ, 161, 480-494 (2005)]

- Quasi-real time coronal MHD simulation using daily-updated SOHO/MDI data.

  http://sun.stanford.edu/~keiji/daily_mhd/daily_mhd.html
- Rather coarse grid $72 \times 32 \times 64$ for the radial, latitudinal and longitudinal direction, respectively
- Polytrope plasma with specific heat ratio of 1.05 $\Rightarrow$ mimic the near-isothermal coronal situation due to the high thermal conduction

More polytropic wind models

[Hayashi, ApJ, 161, 480-494 (2005)]

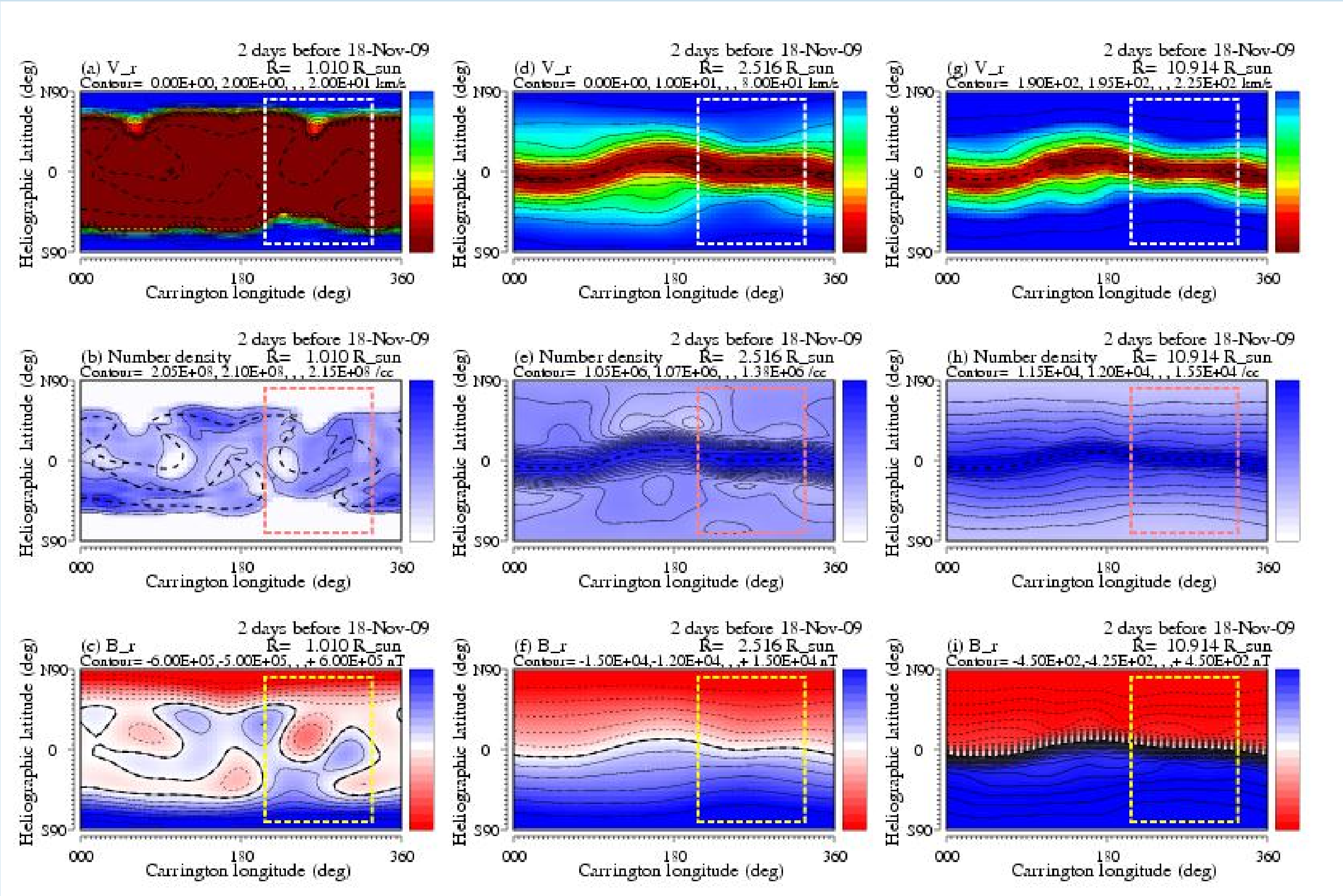

Polytropic assumption: small contrast in flow speed and density (less realistic), but magnetic field quantities and the trends of these plasma variables are well retrieved

A model with variable polytropic index

[Jacobs & Poedts, Adv.Sp.Res 2011]

- Replace the energy equation: $p = K\rho^{\alpha}$.
- Totten et al. (1995) obtained from Helios data fairly polytropic behaviour of the solar wind between 0.3 and 1AU: $\alpha \approx 1.46$ and $K \in [0.5, 50] \times 10^{-22}\mathrm{Nm}^{3\alpha-2}$ dependent on solar wind type.

Polytropic flow: $p = K\rho^{\alpha}$

- $\gamma = \alpha = 1$: isothermal flow
- $\gamma = \alpha$: adiabatic, isentropic flow
- $\gamma \neq \alpha$: $\frac{dp}{dt} - \frac{\gamma p}{\rho}\frac{d\rho}{dt} = (\gamma - \alpha)p\nabla \cdot \vec{v}$.
  Expansion: extra heat will be added to the system if $\alpha < \gamma$.

The radial variation in α and K causes additional acceleration/deceleration of the flow $\Rightarrow$ mimics the unknown physical processes in solar wind acceleration.

A model with variable polytropic index

[Jacobs & Poedts, Adv.Sp.Res 2011]

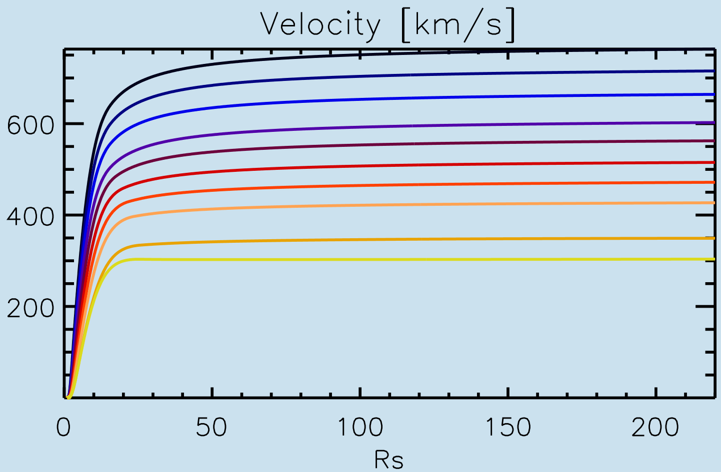

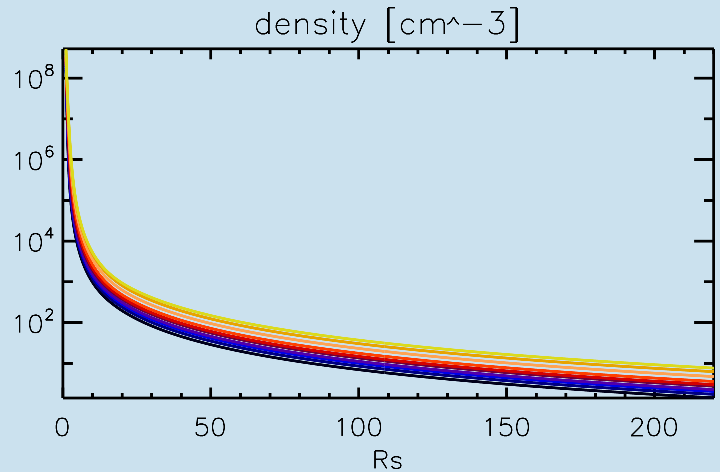

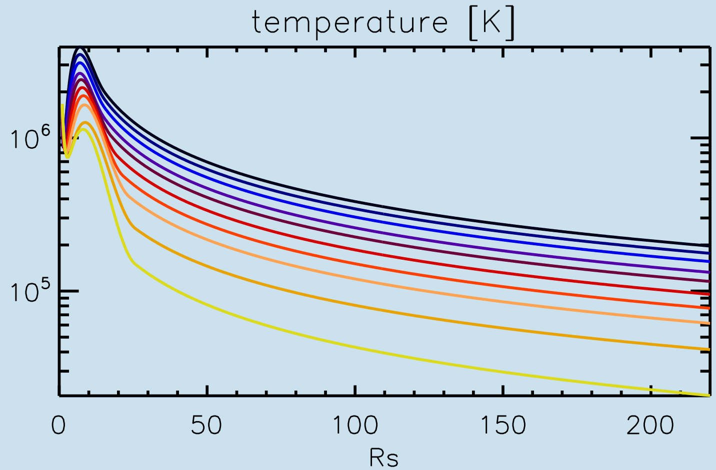

K1AU=53e−22 a1=1.3 a2=1.42 r1=1 r2=15 n0=3e+14 T0=1.25e+6
K1AU=43.7e−22 a1=1.3 a2=1.42 r1=1 r2=15 n0=3.4e+14 T0=1.30e+6
K1AU=36e−22 a1=1.3 a2=1.42 r1=1 r2=15 n0=3.8e+14 T0=1.35e+6
K1AU=29.3e−22 a1=1.3 a2=1.42 r1=1 r2=15 n0=4.2e+14 T0=1.40e+6
K1AU=23.6e−22 a1=1.28 a2=1.42 r1=1 r2=17 n0=4.9e+14 T0=1.475e+6
K1AU=18.7e−22 a1=1.26 a2=1.42 r1=1 r2=19 n0=5.6e+14 T0=1.525e+6
K1AU=14.1e−22 a1=1.24 a2=1.42 r1=1 r2=21 n0=6.3e+14 T0=1.575e+6
K1AU=10e−22 a1=1.22 a2=1.42 r1=1 r2=23 n0=7e+14 T0=1.625e+6
K1AU=6e−22 a1=1.20 a2=1.42 r1=1 r2=25 n0=9e+14 T0=1.65e+6
K1AU=1.4e−22 a1=1.20 a2=1.46 r1=1 r2=25 n0=10e+14 T0=1.65e+6

Example: A polytropic model for solar minimum

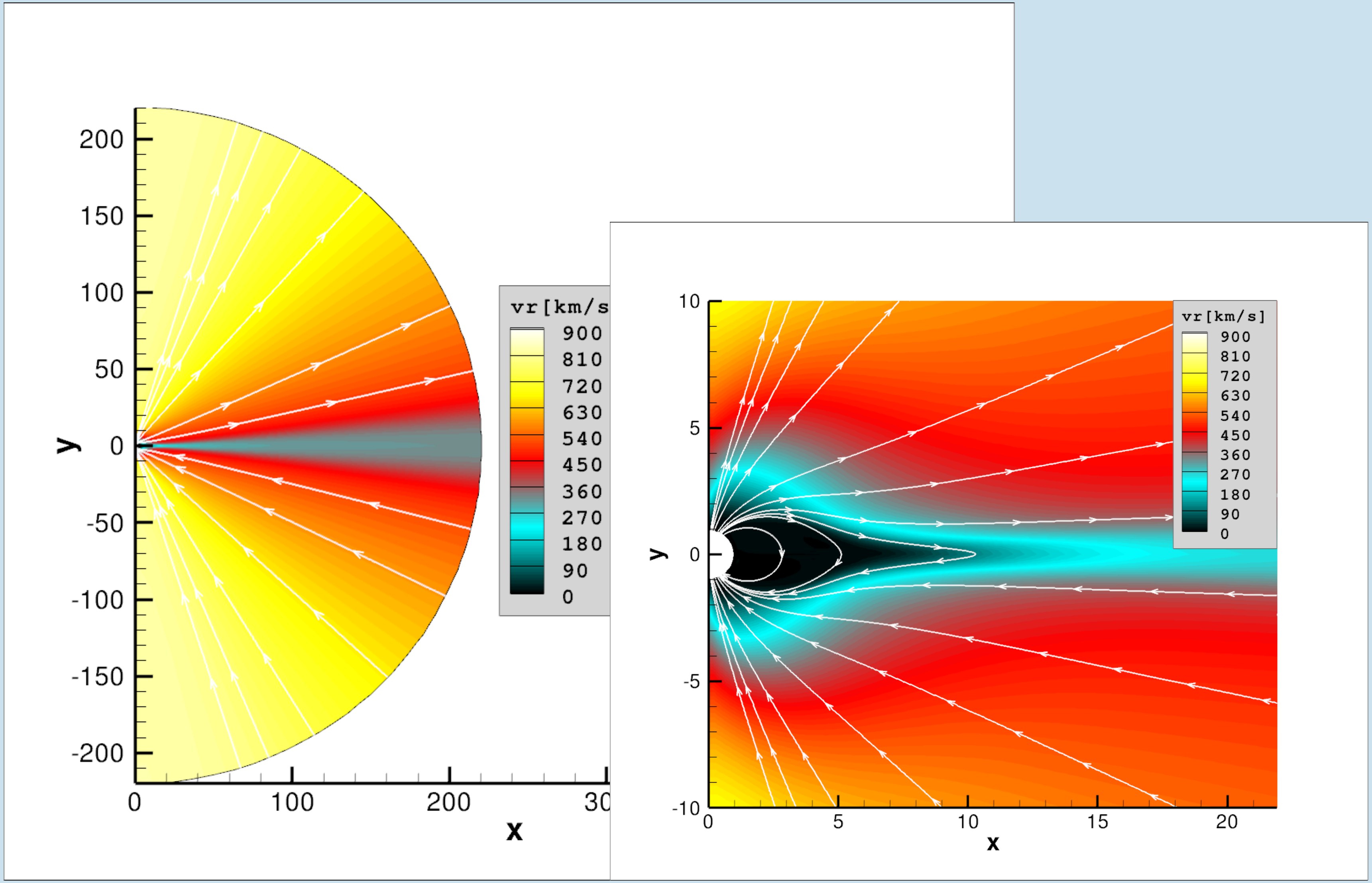

Example: A polytropic model for solar minimum

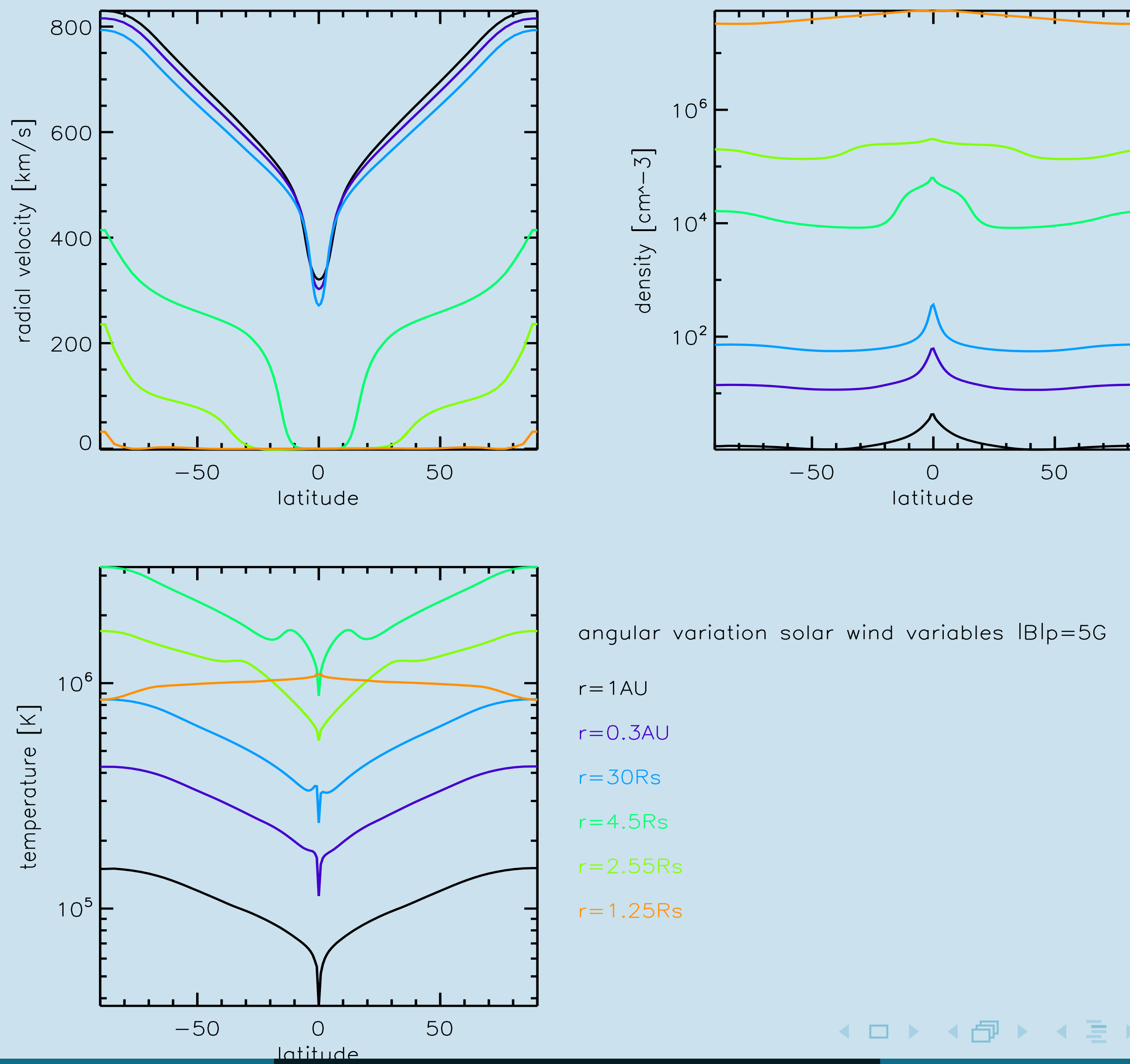

Example: A polytropic model for solar minimum

	V	n_{p+}	T
		pole	
0.3AU	820km/s	17.8cm^{-3}	4.7×10^5K
1AU	837km/s	1.54cm^{-3}	1.68×10^5K
		equator	
0.3AU	374km/s	70cm^{-3}	1.92×10^5K
1AU	387km/s	4.9cm^{-3}	6.3×10^4K

The compressible MHD model of Roussev

[I. Roussev et al., ApJ, 595, L57-L61 (2003)]

- compressible MHD model for steady-state SW.
- initial potential magnetic field is reconstructed throughout the computational volume using the source surface method (magnetogram data as BCs).

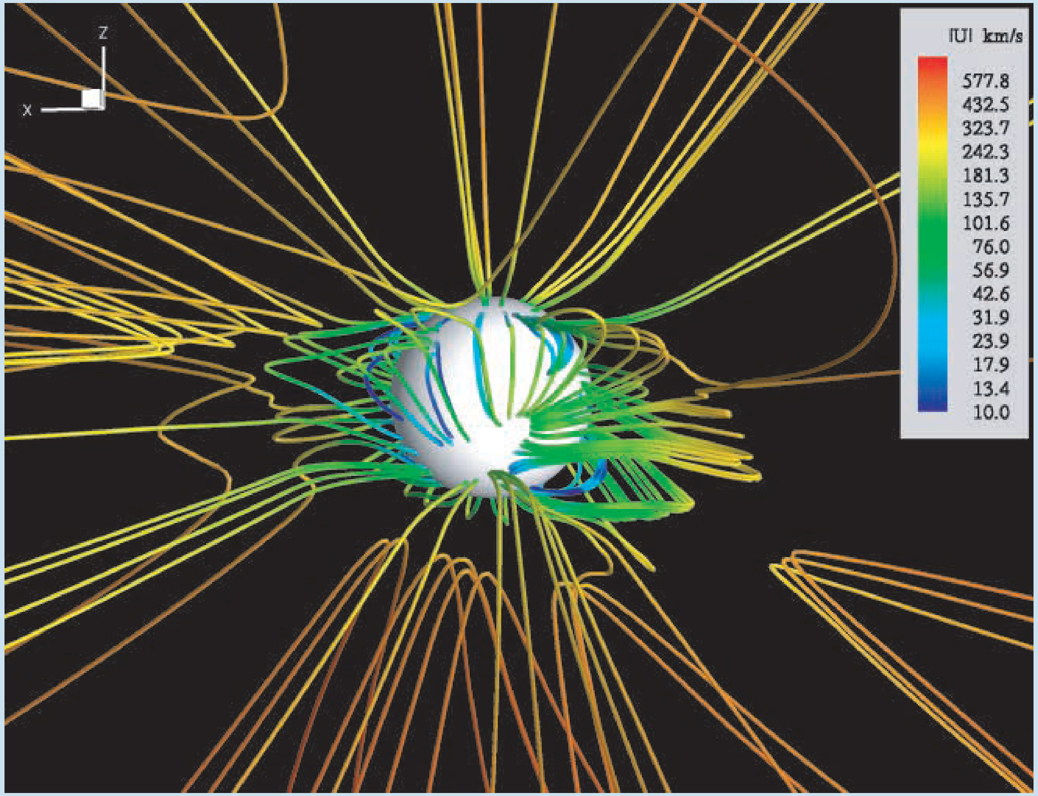

Comparison between Ulysses data normalized to 1 AU (dotted curves in black) and simulation with nontilted, rotating magnetic dipole

The compressible MHD model of Roussev

[I. Roussev et al., ApJ, 595, L57-L61 (2003)]

- compressible MHD model for steady-state SW.
- initial potential magnetic field is reconstructed throughout the computational volume using the source surface method (magnetogram data as BCs).

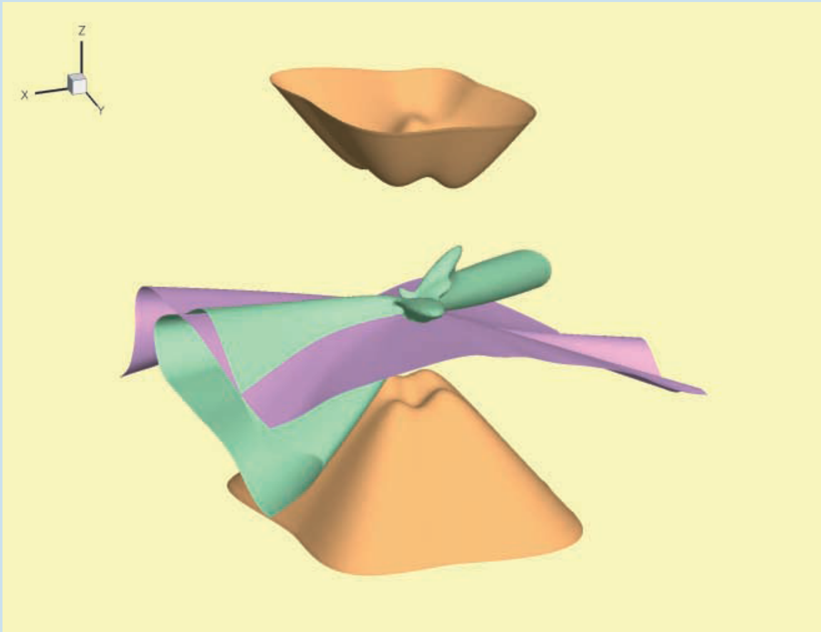

Magnetic field geometry near the Sun

The compressible MHD model of Roussev

[I. Roussev et al., ApJ, 595, L57-L61 (2003)]

- compressible MHD model for steady-state SW.
- initial potential magnetic field is reconstructed throughout the computational volume using the source surface method (magnetogram data as BCs).

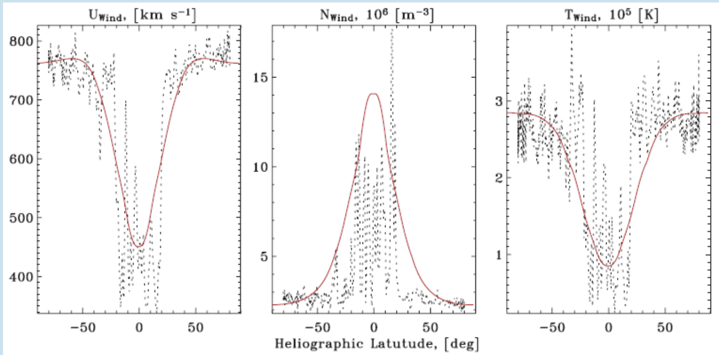

Isosurfaces of a wind speed of 470 km/s (green) and 760 km/s (orange)

- powered by energy interchange plasma - large-scale MHD turbulence.
- thermodynamic quantities are varied with the heliographic latitude and longitude depending on strength radial magnetic field.

Adjustment by Cohen (2007)

[Cohen et al., ApJ, 654, L163-L166 (2007)]

- new compressible MHD model under steady state conditions stemming from the WSA empirical model
- turbulent heating in solar wind is parametrized by phenomenological, thermodynamical model with varied polytropic index

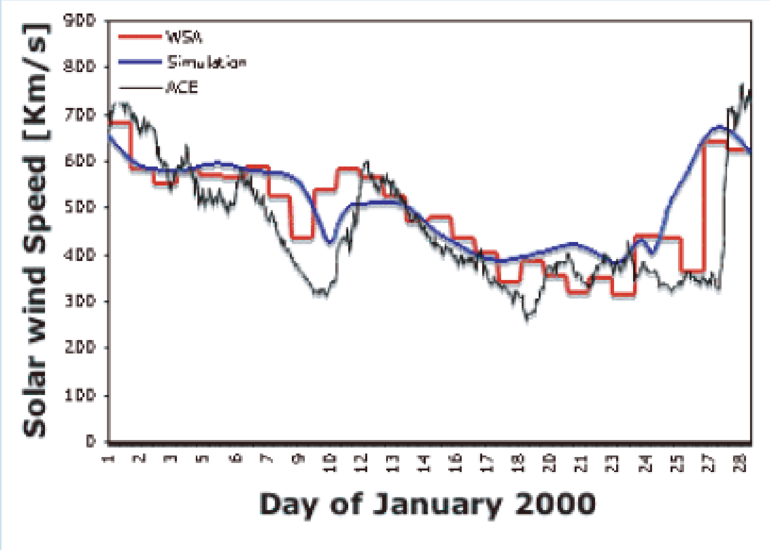

Comparison simulation results (blue) - ACE data (black) - WSA model (red)

Adjustment by Cohen (2007)

[Cohen et al., ApJ, 654, L163-L166 (2007)]

- new compressible MHD model under steady state conditions stemming from the WSA empirical model
- turbulent heating in solar wind is parametrized by phenomenological, thermodynamical model with varied polytropic index

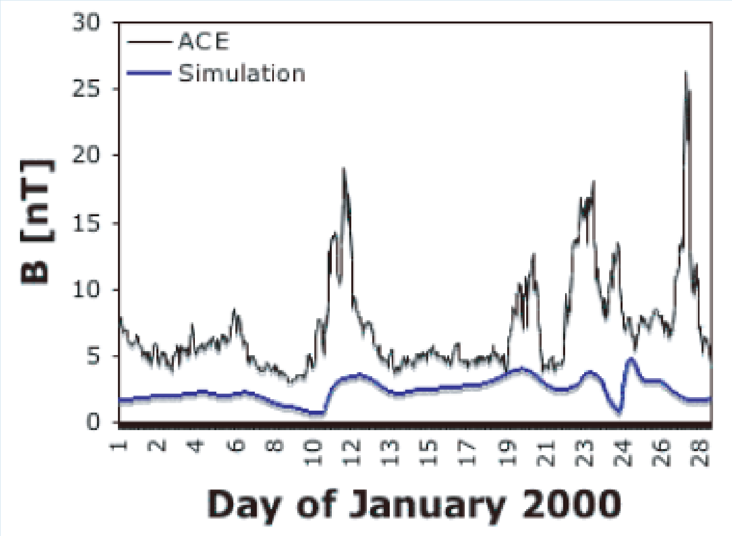

Comparison simulation results (blue) - ACE data (black)

Adjustment by Cohen (2007)

[Cohen et al., ApJ, 654, L163-L166 (2007)]

- new compressible MHD model under steady state conditions stemming from the WSA empirical model
- turbulent heating in solar wind is parametrized by phenomenological, thermodynamical model with varied polytropic index

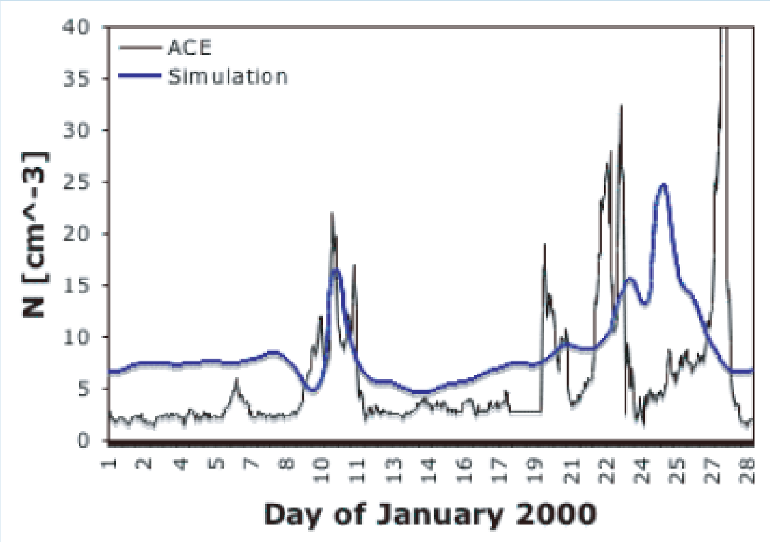

Comparison simulation results (blue) - ACE data (black)

- reproduces the mass flux from Sun to Earth, the temperature structure, and the large-scale structure of the magnetic field.
- input magnetogram needs to be multiplied by a scaling factor.

The 3D MHD model of Nakamizo et al.

[Nakamizo et al., JGR, 114 (2009)]

- Magnetic field is specified by observational data
- Source functions in momentum and energy equations:

$$S_M = M(r-1)\exp(-r/L_M)$$

$$S_E = Q\exp(-r/L_Q) + \nabla\left(\xi T^{2.5}\frac{\nabla T\cdot\mathbf{B}}{B^2}\right)\cdot\mathbf{B}$$

- The absolute values of the source functions are linked with the flux expansion factor of the magnetic field

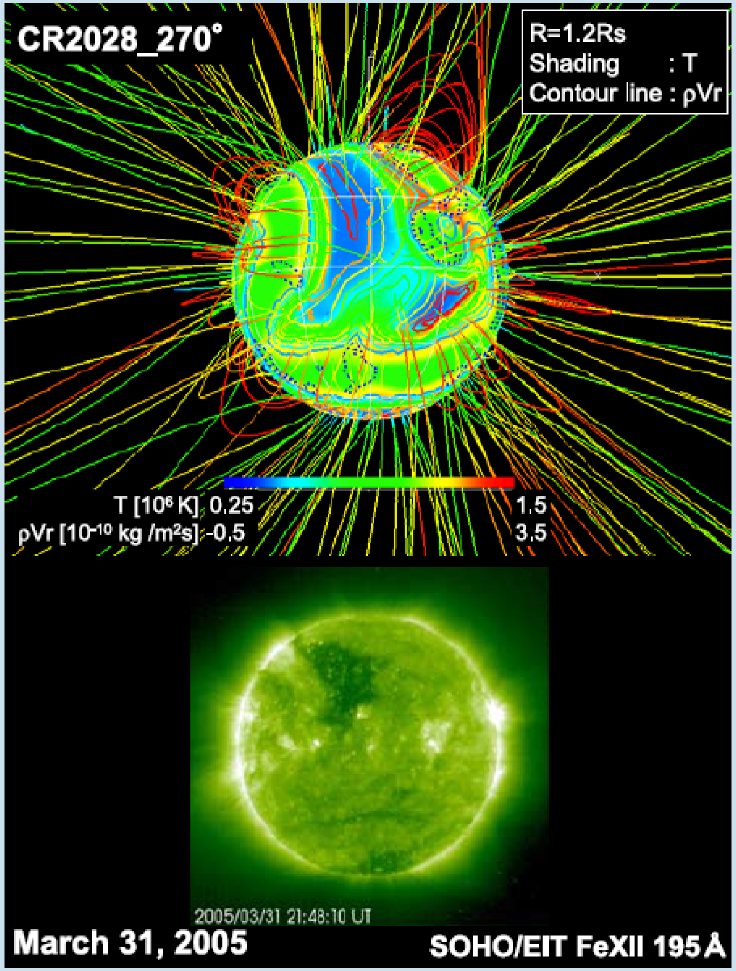

The 3D MHD model of Nakamizo et al.

[Nakamizo et al., JGR, 114 (2009)]

- Magnetic field is specified by observational data
- Source functions in momentum and energy equations:

$$S_M = M(r-1)\exp(-r/L_M)$$

$$S_E = Q\exp(-r/L_Q) + \nabla\left(\xi T^{2.5}\frac{\nabla T \cdot \mathbf{B}}{B^2}\right.$$

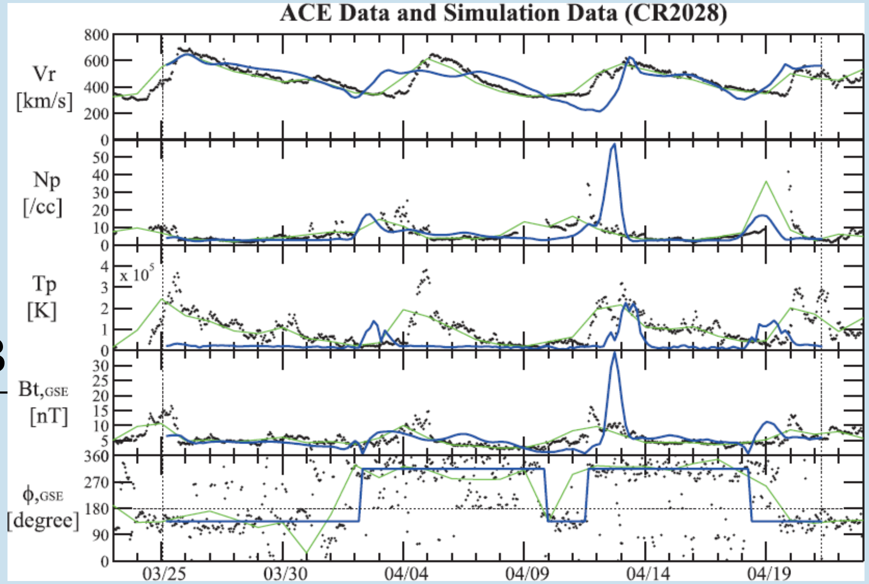

- The absolute values of the source functions are linked with the flux expansion factor of the magnetic field

A solar wind model with Alfvén waves

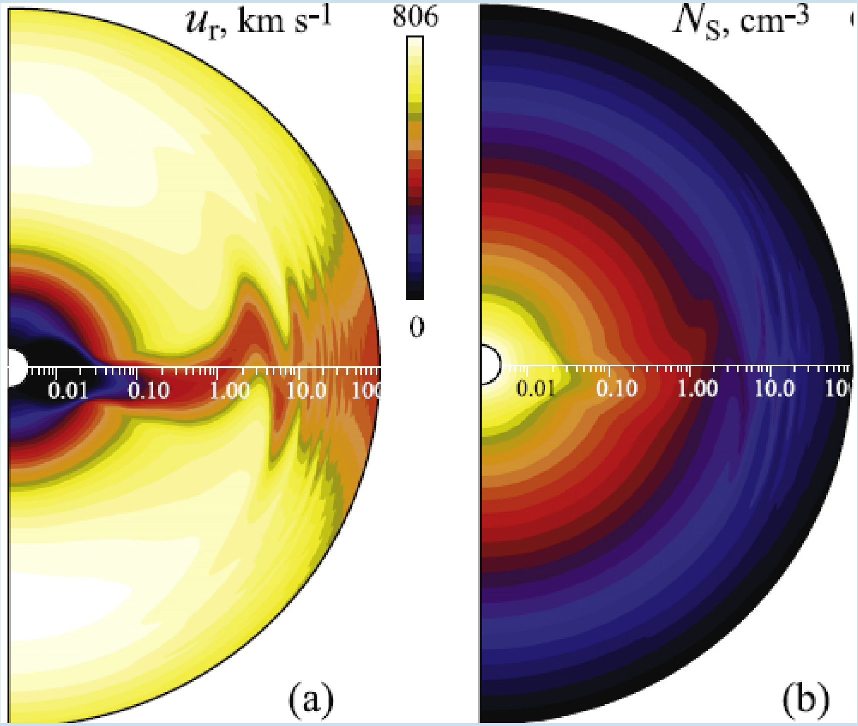

[Usmanov & Goldstein, JGR, 111 (2006)]

- 3D MHD model.
- Covers the region from the coronal base to 100 AU.
- Addition of **Alfvén wave momentum and energy** in the WKB approximation.

$$\frac{\partial \mathcal{E}}{\partial t}+\nabla\cdot[(\mathbf{v}+\mathbf{v}_A)\mathcal{E}] = -\frac{\mathcal{E}}{2}\nabla\cdot\mathbf{v}-|\mathbf{v}+\mathbf{v}_A|\frac{\mathcal{E}}{L}$$

- Inclusion of the effect of pickup ions in the distant heliosphere.

pickup ions = interstellar H atoms becoming ionized (thus sensitive to the IP magn.field) as a result of charge exchange with solar wind protons and photoionization by solar radiation.

A two-temperature solar wind model

[van der Holst et al., ApJ, 725 (2010)]

- 3D MHD model, $T_p \neq T_e$.
- anisotropic heat conduction of the electrons.
- acceleration by Alfvén waves.
- inner boundary conditions from observations and an empirical model (WSA): spatial varying density and temperature; magnetogram data during absolute minimum conditions.

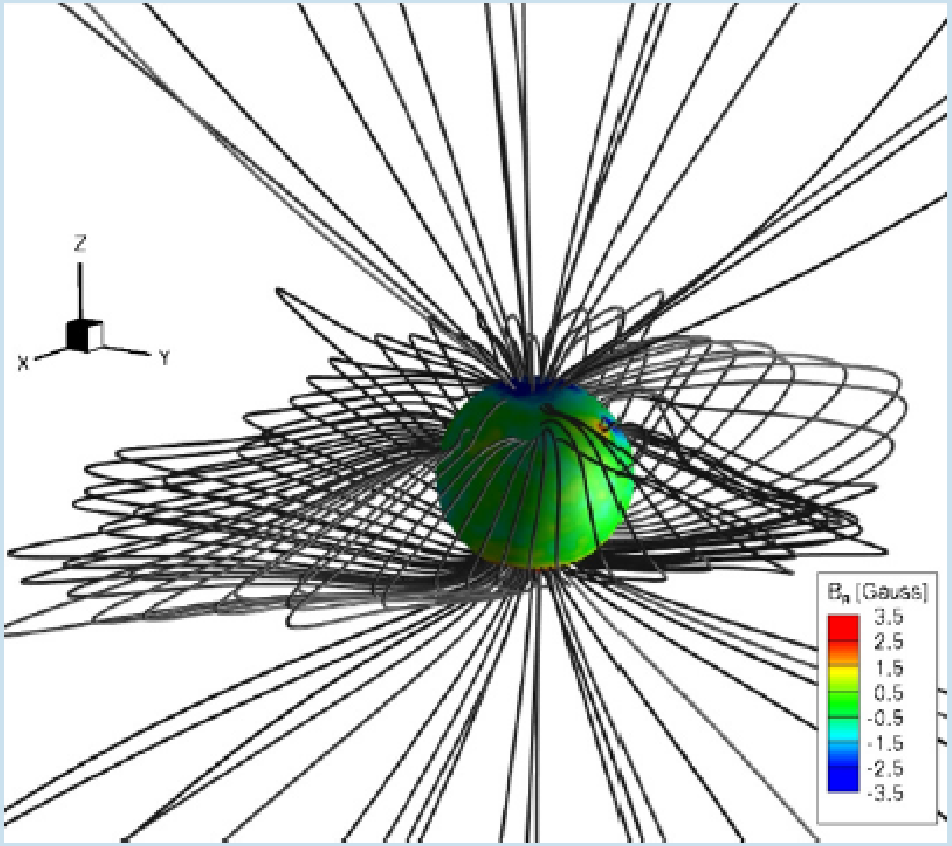

3D magnetic field topology showing helmet streamer and coronal hole (CR2077)

A two-temperature solar wind model

[van der Holst et al., ApJ, 725 (2010)]

- 3D MHD model, $T_p \neq T_e$.
- anisotropic heat conduction of the electrons.
- acceleration by Alfvén waves.
- inner boundary conditions from observations and an empirical model (WSA): spatial varying density and temperature; magnetogram data during absolute minimum conditions.

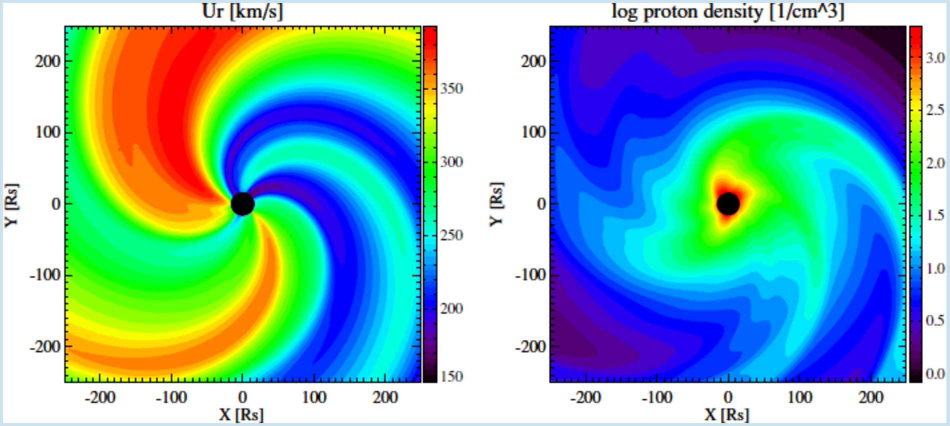

slow and fast speed streams in the equatorial plane.

A two-temperature solar wind model

[van der Holst et al., ApJ, 725 (2010)]

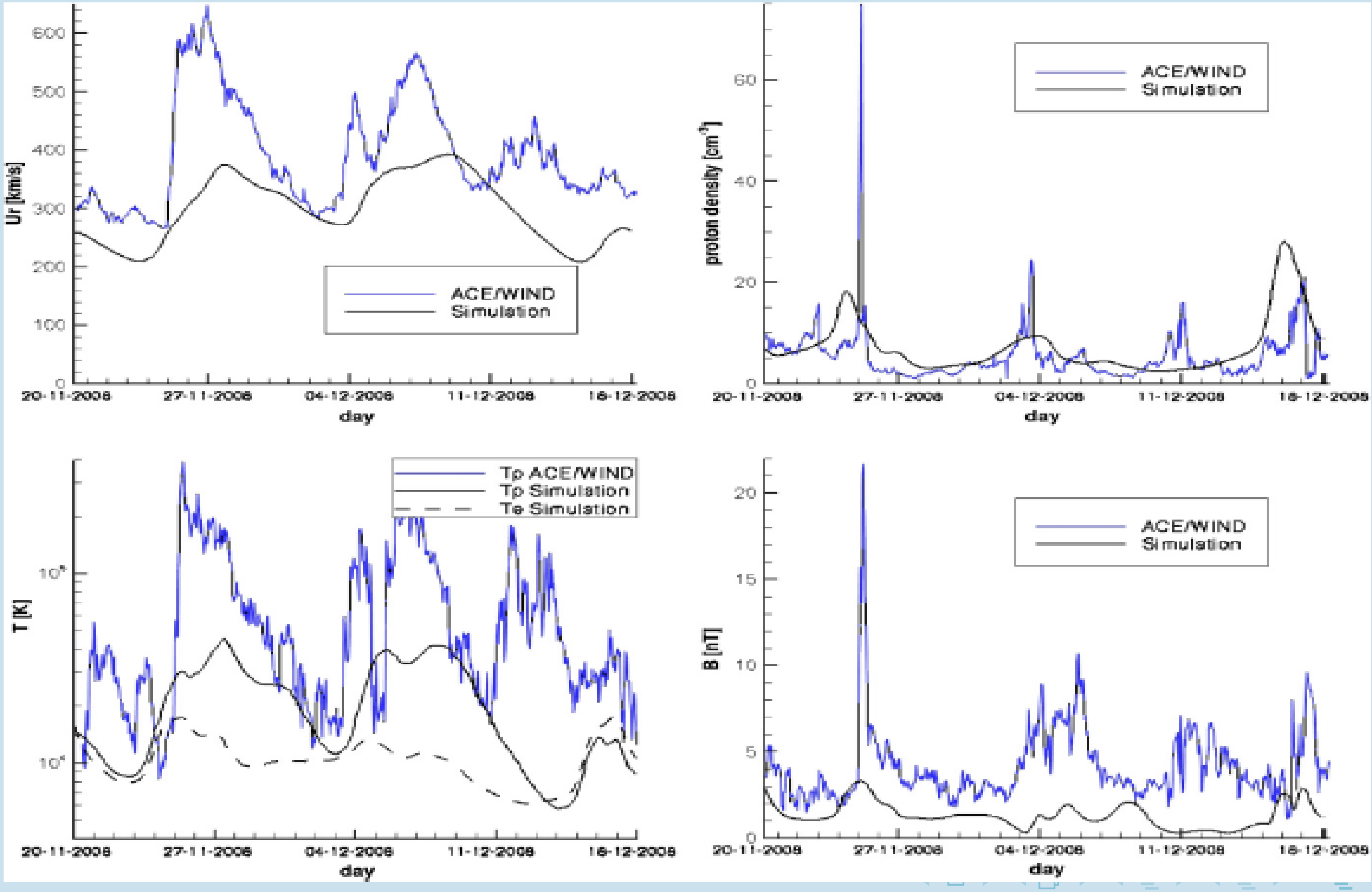

A realistic model for the lower solar corona

[Lionello et al., ApJ (2009); Downs et al., ApJ (2010)]

In order to study the fine structure of the corona it is essential to include the transition region $\rightarrow$ addition thermodynamics terms.

$$\frac{\partial E}{\partial t} + \nabla \cdot (\mathbf{F}_{MHD} + \mathbf{F}_C) = Q_{MHD} + Q_r + Q_h$$

- $\mathbf{F}_C = -\kappa_0 T^{5/2}\mathbf{B}(\mathbf{B} \cdot \nabla T)$.
- $Q_r = -n_e n_p \Lambda(T)$
- Q_h: empirical heating function.

Boundary conditions:

- chromospheric boundary: resolve the entire transition region.
- radiative energy balance model: start at top of transition region; density is function of the physics included in the model.

A realistic model for the lower solar corona

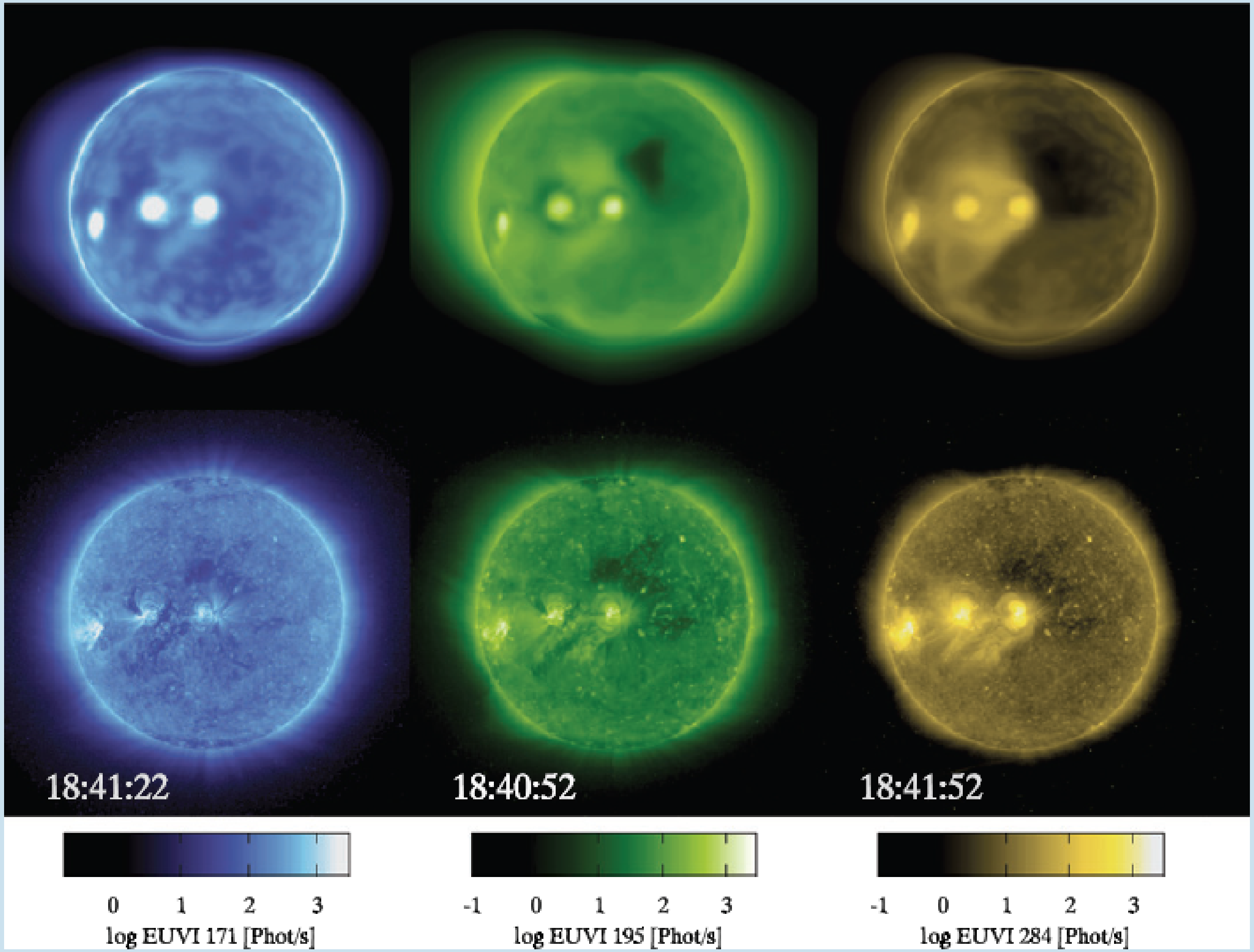

Comparison between simulated corona (top) and 2008 March 25 EUVI-A images. (Downs et al. 2011)

A realistic model for the lower solar corona

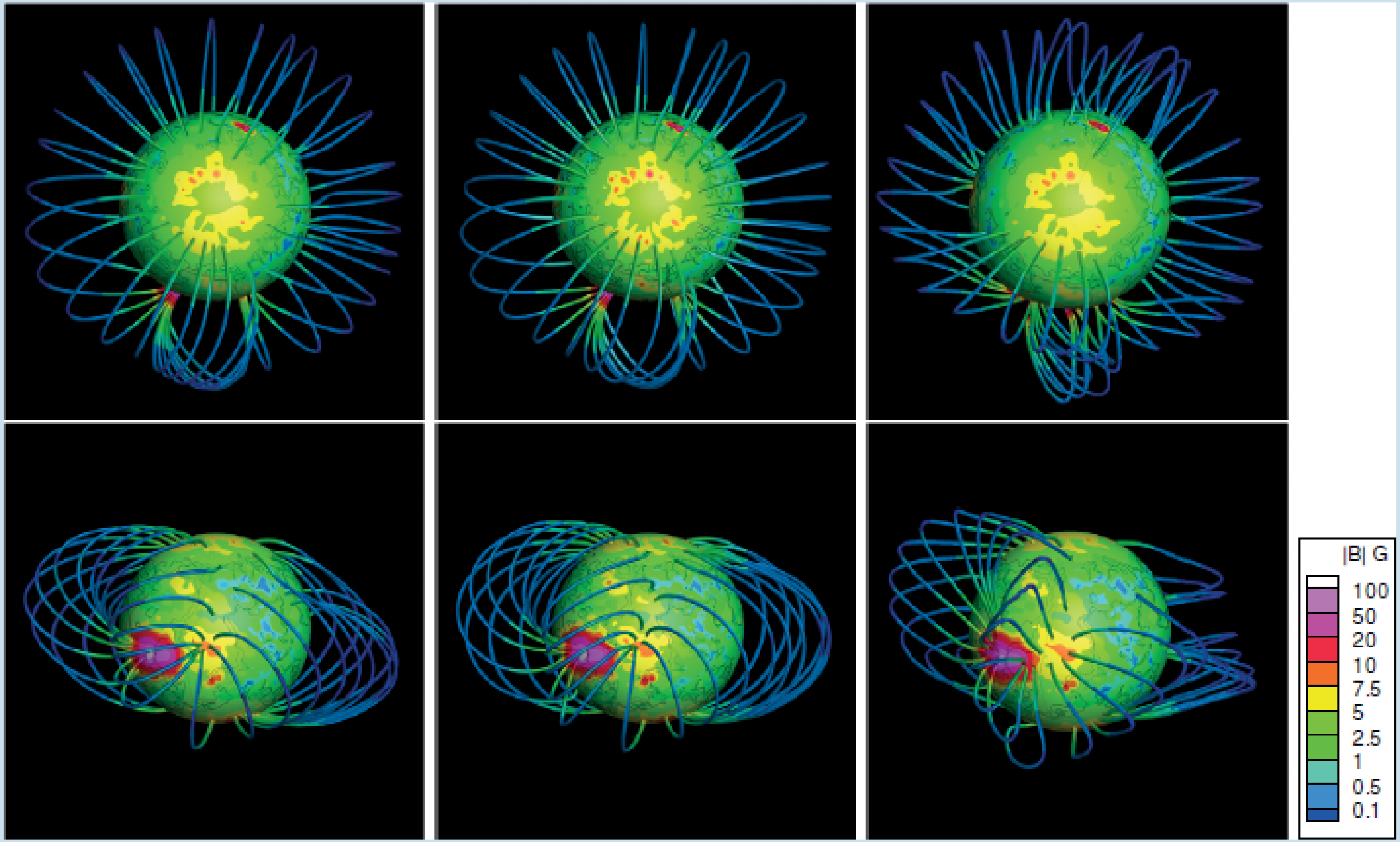

Left: PFSS extrapolation, Right: realistic coronal model (Downs et al. 2010).

Multi-fluid modelling

[Ofman, JGR (2004); Ofman et al., ApJ (2011)]

Global, single fluid models can reproduce the general magnetic structure, but not the distinct dynamics of the different species.

- 3-fluid MHD model: the electrons, protons, and heavy ions can be modeled as coupled magnetized fluids using MHD-like equations.
- Contains important physical processes:
  - collisional and electromagnetic coupling between the various fluids.
  - different heating and acceleration processes for the electrons, protons, and heavy ions.
  - thermal conduction is neglected, instead polytropic assumption $\gamma = 1.05$.
  - empirical heating term.
- 2.5D

Multi-fluid modelling

[Ofman, JGR (2004); Ofman et al., ApJ (2011)]

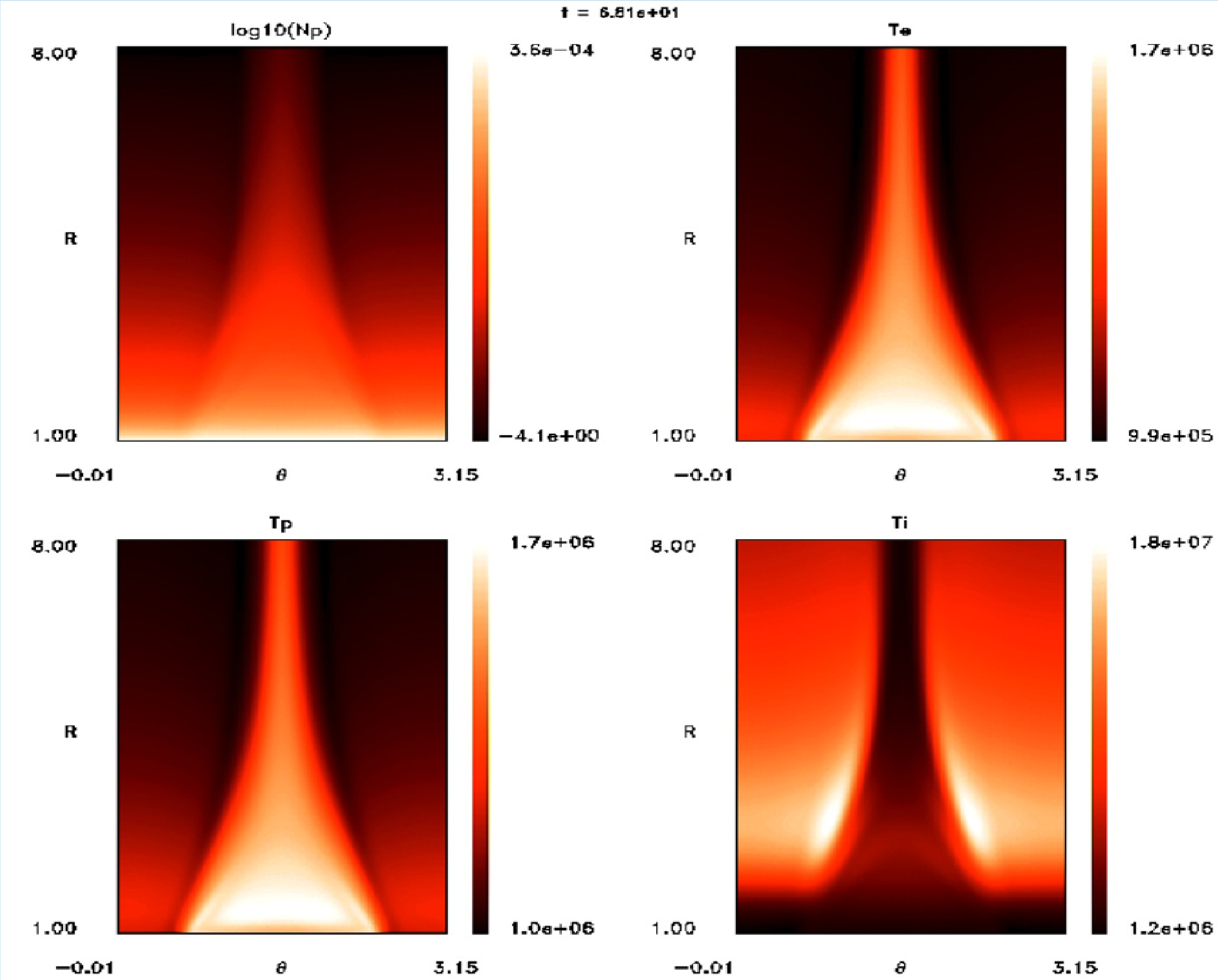

Streamer density structures, and temperatures of protons, electrons, and O^{5+} ions.

Ofman et al. 2011

Multi-fluid modelling

[Ofman, JGR (2004); Ofman et al., ApJ (2011)]

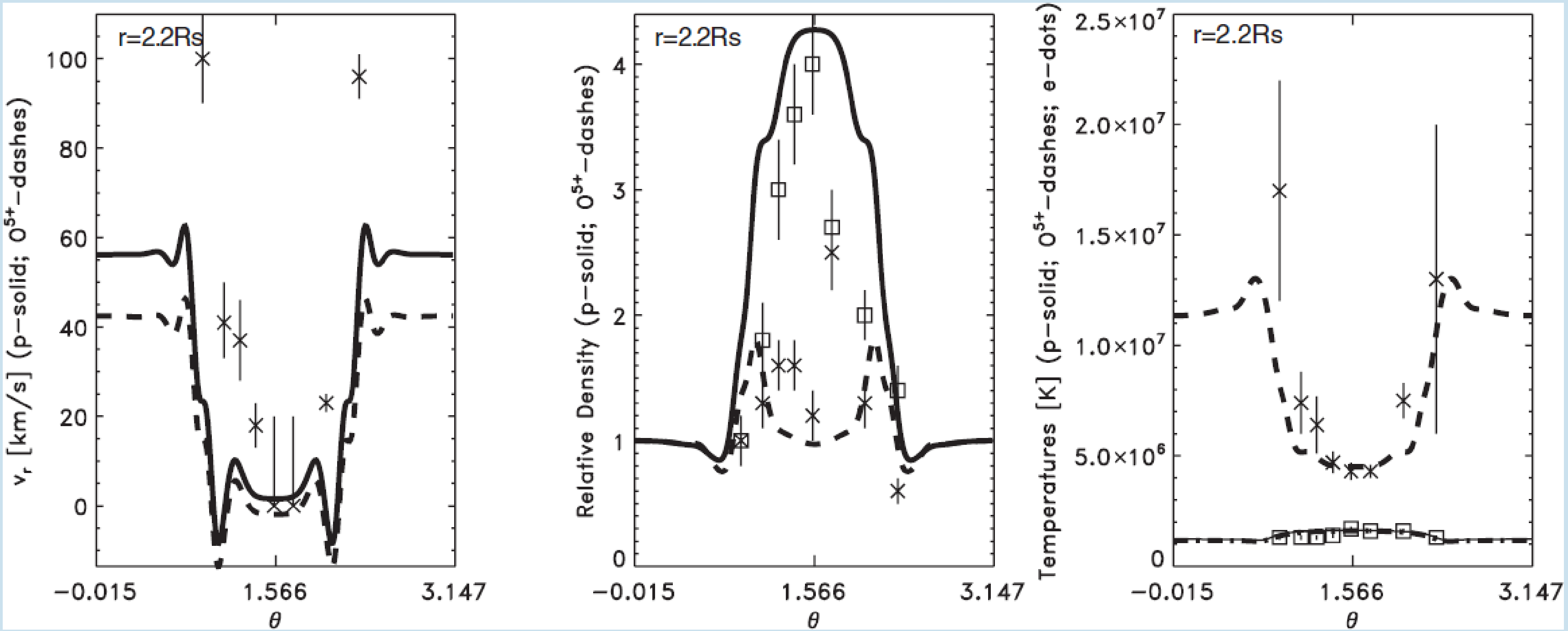

θ-dependence of the velocity, temperature and density at $2.2R_\odot$. Comparison with observations on August 29, 1996 (crosses O^{5+} ions, squares neutral hydrogen). Ofman et al. 2011

An exospheric model [Lamy et al., JGR (2003,2004)]

- Exobase: region where collisions between particles can be neglected.
- Kinetic, collisionless model - 1D - radial magnetic field - no wave-particle interactions
- In the exosphere:
  $E = mv^2/2 + m\phi_g + ZeV(r) = cst$
  m particle mass, v velocity, ϕ_g gravitational potential, Ze charge, $V(r)$ IP electrostatic potential.
- Non-Maxwellian velocity-distribution function (instead: kappa-function).
- Can be applied to electrons, protons, and heavy ions.
- Result depends strongly on $V(r)$.

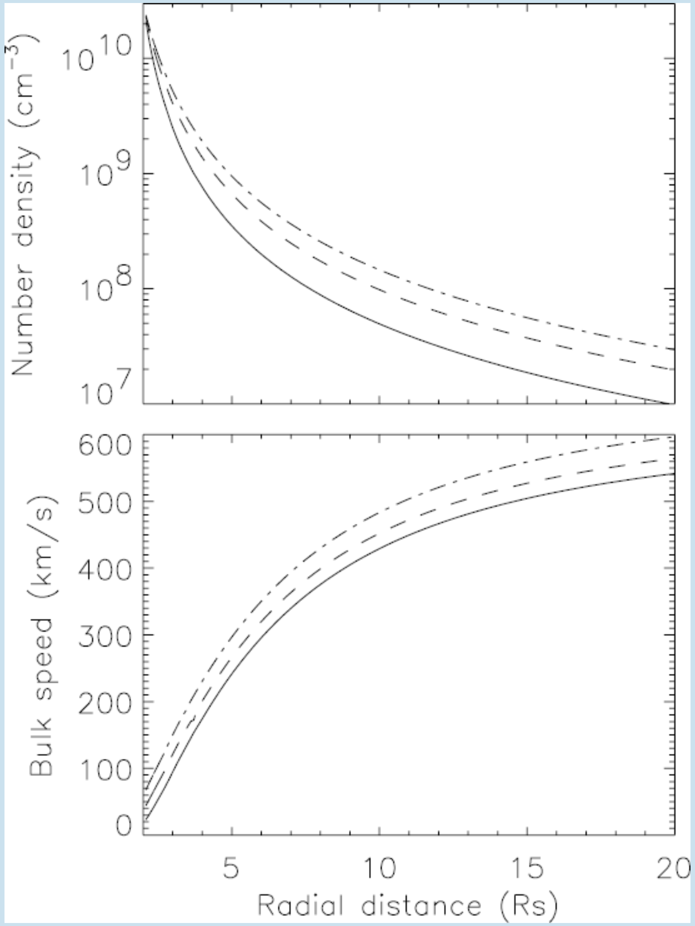

collisionless kinetic theory is able to reproduce the large bulk velocities observed in the fast solar wind, without ad hoc assumptions of hydrodynamical/fluid models.

Outline

Conclusions

- **Solar wind modeling is very important** $\rightarrow$ essential for space weather forecasting.
- most models are **based on MHD**, but
  - energy equation replaced by **polytropic relation**.
  - **including source terms** to mimic bimodal features
  - often **neglecting important physics** (like electric conduction) to save CPU.

  $\Rightarrow$ good qualitative results!, but *often poor quantitative agreement*
- *multi-fluid and kinetic effects are important!* $\Rightarrow$ needed for **self-consistent models** providing real physical insights (avoiding artificial source terms).
- Large gap between small scale (kinetic) models and large scale (fluid) models.

The End